



MASTERARBEIT

Titel der Masterarbeit

Molecular characterization of lipid droplet associated
proteins in the chicken yolk sac

Verfasser

Thomas Finkes BSc

angestrebter akademischer Grad

Master of Science (MSc)

Wien, 2012

Studienkennzahl lt. Studienblatt: A 066 834

Studienrichtung lt. Studienblatt: Masterstudium Molekulare Biologie

Betreuerin / Betreuer: O. Univ. Prof. DI. Dr. Wolfgang J. Schneider

Directory

1. INTRODUCTION.....	4
1.1 The chicken (<i>Gallus gallus domesticus</i>) as a model organism	4
1.2 Chicken yolk sac (YS)	5
1.3 Lipid droplets (LDs).....	7
1.4 PERILIPINS.....	10
1.4.1 PLIN1	11
1.4.2 PLIN2.....	13
1.4.3 PLIN3.....	16
1.4.4 PLIN4.....	17
1.4.5 PLIN5.....	17
1.5 Lipases	19
1.5.1 ATGL (Adipose triglyceride lipase)	19
1.5.2 PNPLA3 (Patatin-like phospholipase domain-containing protein)	20
1.5.3 LAL (Lysosomal acid lipase).....	21
1.5.4 HTGL (Hepatic triglyceride lipase)	22
1.5.5 LPL (Lipoprotein lipase).....	22
2. MATERIALS AND METHODS	24
2.1 Chemicals and Enzymes.....	24
2.2 Bacterial strains and vector systems	24
2.3 Oligonucleotide primers	26
2.4 Animals.....	26
2.5 Dissection of chicken yolk sac layers	26
2.6 Molecular biological methods: RNA.....	27
2.6.1 Total RNA extraction from chicken yolk sac tissue	27
2.6.2 Reverse Transcription of isolated RNA	28
2.7 Molecular Biological Methods: DNA.....	28
2.7.1 Reverse transcriptase polymerase chain reaction (RT-PCR).....	28
2.7.2 Agarose gel-electrophoresis	29
2.7.3 Agarose gel extraction	30
2.7.4 DNA ligation.....	31
2.7.5 Production of chemical competent E. coli TOP10.....	31
2.7.6 Transformation of chemical competent E. coli	32
2.7.7 Mini preparation of Plasmid DNA	32
2.7.8 Midi preparation of Plasmid DNA	33
2.7.9 Restriction enzyme (RE) digestion	34
2.7.10 QPCR (Quantitative real time polymerase chain reaction)	34
2.8 Molecular Biological Methods: Protein	35

2.8.1	Protein Extraction: Whole TRITON X-100 tissue-extract preparation	35
2.8.2	Preparation of Triton X-100 membrane-protein extracts	36
2.8.3	Protein concentration measurement	36
2.8.4	Western blot analysis	38
2.8.5	Protein isolation from cellular lipid fractions by subcellular fractionation	39
2.8.6	Subcellular fractionation method 2	39
2.8.7	Processing of the cytosolic protein fraction	40
2.9	Cultivation of EECs of the area vitellina	41
2.10	Immunofluorescence experiments	41
2.11	Utilized antibodies and antisera in Western blotting.....	42
2.12	Utilized antibodies, antisera, and preimmune sera (PI) in immunofluorescence experiments.....	42
3.	RESULTS	43
3.1	Investigation of PLIN gene expression in chicken tissues	43
3.2	Investigation of PLIN2 protein levels in the yolk sac.	48
3.3	Immunofluorescence: PLIN2 antibody staining in area vitellina EECs	51
3.4	Immunofluorescence: PI staining in area vitellina EECs	54
3.5	Lipases involved in the mobilization of TGs in the chicken yolk sac	57
3.6	Investigation of lipase protein levels in the yolk sac.....	61
4.	DISCUSSION.....	63
5.	REFERENCES	67
6.	LIST OF ABBREVIATIONS.....	75
	ABSTRACT	81
	ZUSAMMENFASSUNG	83
	ACKNOWLEDGEMENTS	85
	CURRICULUM VITAE.....	86

1. Introduction

1.1 The chicken (*Gallus gallus domesticus*) as a model organism

The domestic chicken (*Gallus gallus domesticus*), termed as domestic fowl is a descendent of the red jungle fowl. It was domesticated from the red jungle fowl approximately 6000 before Christ in the area of today's Vietnam and Thailand and was widespread from there over the globe (Komiyama et al., 2004). The domesticated chicken was used for many centuries simply as food resource before it was discovered to be an excellent model organism. As the domestic chicken is oviparous, the eased access to the embryo can be used for early vertebrate developmental studies (Stern, 2005). Many famous scientists have selected the domestic chicken for their works. Already in the third century Before Christ (BC) the philosophe Aristotle utilized *Gallus gallus domesticus* for first embryological studies. In the late 19th century Charles Darwin studied the breeding behaviour of domestic chickens (Darwin, C. 1868, *The Variation of Plants and Animals under Domestication* John Murray, London UK). Later in that century the chemist Louis Pasteur executed infection studies with chickens to find a vaccine against fowl cholera (Pasteur, *The Attenuation of the Causal Agent of Fowl Cholera* 1880). In other fields like immunology and medicine the model organism chicken pioneered with the discovery of B-cells and the isolation of the first oncogene (Brown, et al., 2003).

The chicken genome has a size of 1.1×10^9 base pairs (bp). The genome is divided on 39 chromosomes, 30 microchromosomes and 9 pairs of macrochromosomes (Ladjali-Mohammedi et al., 1999). Birds follow a ZW sex-determination system compared to the XY system in mammals and the XO system in many insects. Males are homogametic (ZZ), while females are heterogametic (ZW). The Z chromosome is, compared to the mammalian X chromosome far bigger than the W chromosome. The chicken genome consists of remarkably low amounts of repetitive sequences, only 11% compared to approximately 50% in mammals which makes it a favorable model for genomic studies.

Nowadays two different breeds of domestic chicken are available. The first one, called meat-breed grows fast and reaches a weight of 2.3kg at an age of 6 weeks. If not food restricted it gets obese at maturity. The second one, the laying breed grows slower and reaches a weight of 2.3kg at maturity. Hence the nonexistent weight problem the laying breed is favored for scientific use. The most common used laying breeds originate from the white Leghorn strain. Generally the white Leghorn reaches maturity at 5 month and achieves the highest laying rates in the first year (Bahr, *Sourcebook of Models for Biomedical Research*, edited by Conn, 2008).

1.2 Chicken yolk sac (YS)

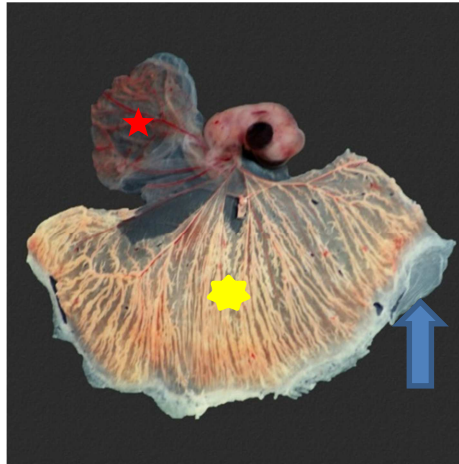


Figure 1. 5 day (d) chicken embryo with YS (yellow asterisk) and allantois (red asterisk). The completely un-vascularized EECs of the area vitellina are indicated with the blue arrow. The egg was incubated for 5d post laying at 37°C in an incubator. Picture was kindly provided by Raimund Bauer.

The chicken YS is an extra embryonic membranous sac attached to the embryo. It encloses the eggs' yolk and mediates the transfer of nutrients from the yolk to the embryo. Yolk remnants that are not used by the embryo before hatching are drawn into the abdomen at embryonic day 19 providing nourishment for the first 2-3 days.

The YS consists of all three germ layers. The outer part of the YS, most distal to the yolk, is the ectoderm. It is exposed to the egg albumen and is continuous with the embryo's ectoderm (Nakazawa, et al., 2011). The YS mesoderm lies beneath the ectoderm. It is made up by vascular endothelial cells, blood cells and smooth muscle cells. It is the place of early YS erythropoiesis (Sheng, 2010). The innermost part of the YS is represented by the endodermal layer. It builds up an epithelial sheet; hence cells of the endoderm are called endodermal epithelial cells (EECs). EECs lie at the apical site of the YS, in direct contact to the yolk. These EECs indirectly supply nutrients from the yolk for the embryo (Mobbs and McMillan, 1981; Speake et al., 1998). The yolk generally is composed of approximately 50% water, 15% protein, 33% fat, and 1% carbohydrates. Dependent on egg weight, strain and hen age the division of components can vary (Shenstone, 1968; O'Sullivan et al., 1991; Vieira and Moran, 1998).

In the early stages (earlier than 10d post laying) the YS can be clearly divided into two distinct differentiated regions called area vasculosa and area vitellina (Fig. 1). Both areas are

composed of EECs. In contrast to the area vasculosa, the area vitellina is not overgrown with a blood vessel layer of mesodermal origin. With ongoing growth, development, and differentiation of the YS the area vitellina gradually “transforms” into the area vasculosa, as the mesodermal blood vessel layer overgrows the area vitellina.

The molecular mechanism that underlies the uptake of nutrients from the yolk is not completely understood but it is thought that the EECs of the chicken YS work as a kind of digestive system. Nutrients from the yolk are taken up, broken down and rebuilt before the release to the mesodermal blood vessels (Fig. 3). In particular the fatty compounds are taken up by non-specific phagocytosis at the apical surface of the EECs of the YS membrane (Speake et al., 1998). In figure 3 (Nakazawa, et al., 2011), a schematic view is given of how EECs of the area vasculosa of early embryonic stages function and interact with the mesodermal blood vessels. From the apical side of the EECs proteins, lipoproteins and lipids are taken up from the yolk. When the nutrients are taken up in coated vesicles they are transferred to the apical vacuole where likely their breakdown occurs. In the next step, in a bigger compartment, the yolk droplet, further breakdown and subsequent resynthesis of nutrients takes place. In the last step lipoproteins, cardiovascular regulators and other serum proteins are delivered to the vascular lumen of the mesodermal blood vessel cells. As described in more detail in the Results section, I found EECs of the area vitellina of the chicken YS containing large amounts of lipid droplets (LDs) (Fig. 2).

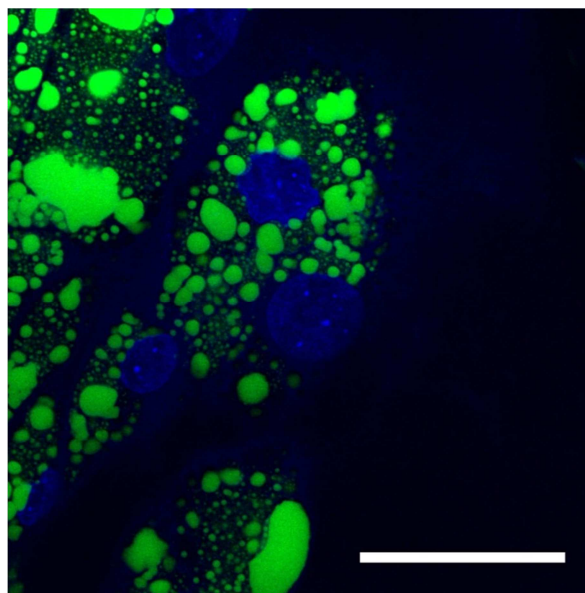


Figure 2. EECs of the area vitellina in the 5d chicken YS. The cells are filled with LDs (as shown by green BODIPY 493/503 fluorescence). Nuclei (DAPI staining) are shown in blue. Scale bar; 50 μ m.

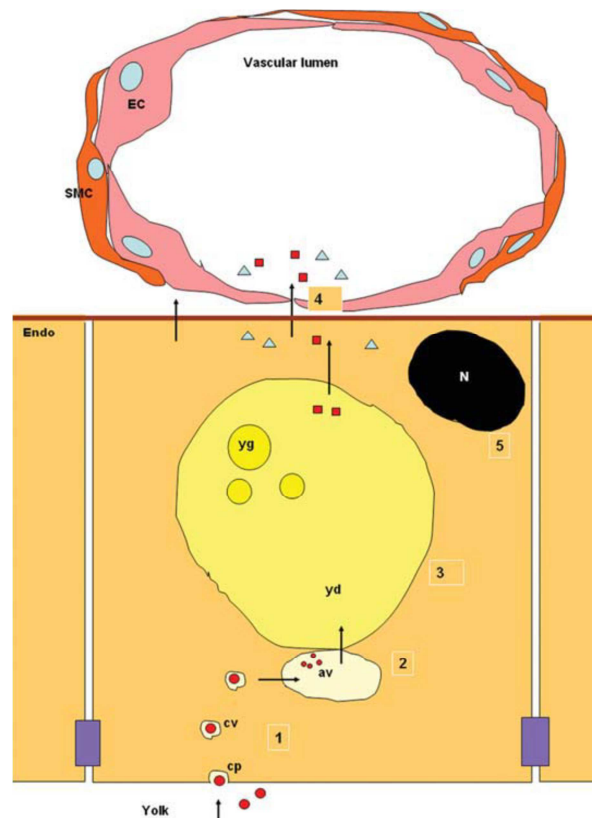


Figure 3. Scheme of yolk nutrient uptake by EECs of the embryonic chicken YS to the mesodermal blood vessel layer. Abbreviations: av: apical vacuole; cp: coated pit; cv: coated vesicle; EC: endothelial cell; Endo: YS endoderm; SMC: smooth muscle; N: nucleus; yd: yolk drop; yg: yolk granule; The figure was taken from Nakazawa, et al., 2011.

1.3 Lipid droplets (LDs)

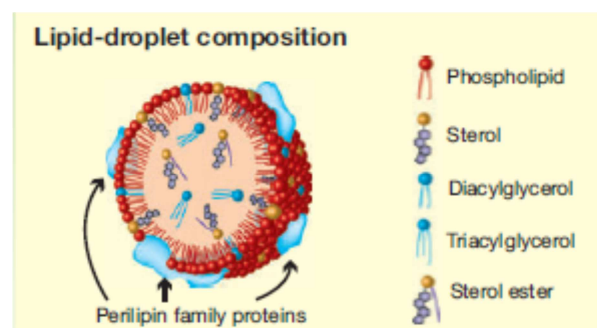


Figure 4. This figure shows the schematic structure of a LD. A phospholipid monolayer surrounds the neutral lipid core that comprises sterol ester and triacylglycerol. The figure was taken from Guo et al., 2009.

Lipid droplets are the major fat depots of cells. They have a globular shape and are bounded by a phospholipid monolayer (Fig. 4). The most abundant phospholipid in the membrane of LDs is phosphatidyl choline (Tauchi-Sato, et al., 2002). Depending on the cell type they vary in size from 0.1 μ m to 2 μ m in most mammalian cells and occupy approximately 3% of the cytosol. In adipocytes LDs can reach a diameter of 150 μ m and can occupy up to 90% of the cytosol (Pilch et al., 2007). Their main purpose is to store excess fatty acids like TGs and sterols in form of neutral lipids (esters) in a hydrophobic core. Storage of excess free fatty acids (FFAs) is of great importance especially in non-adipose tissue. If the storage is impaired a phenomenon called lipotoxicity can occur. In many studies it was shown that accumulation of excess FFAs in liver, kidney, heart, and skeletal muscle can cause heart failure, diabetes typ II, atherosclerosis, and obesity (Schaffer, 2003).

Large amounts of neutral lipids stored in LDs of adipocytes are mostly utilized for skeletal muscles, which by themselves are able to store remarkable amounts of neutral lipids in form of LDs. In steroidogenic cells like testes and ovaries the stored sterols are used for steroid hormone synthesis. Other tissues like liver, intestine, kidney, and heart also contain small intracellular LDs (Hammersen, F. (1985) *Histology: Color Atlas of Microscopic Anatomy*, 2nd Ed., Urban & Schwarzenberg, Baltimore). Stored CEs in these tissues provide a source for membrane synthesis.

Before LDs can form, the neutral core lipids have to be gathered. In a first step FFAs have to be released from their extracellular transporters, the lipoproteins. Lipoprotein lipase (LPL), which acts on the surface of capillary endothelial cells, selectively cleaves off FFAs from bound TG-rich lipoprotein particles. Then the FFAs enter the cells via passive diffusion accelerated by e. g. fatty acid translocase (Ehehalt et al., 2006). Additionally, FFAs can also be synthesized in cells from carbohydrates. Subsequently, FFAs conjugate with Coenzyme A (CoA) to form fatty acyl-CoA. Those fatty acyl CoA molecules are then converted to diacylglycerides by glycerol-3-phosphate acyltransferase and sn-1-acylglycerol-3-phosphate acyltransferase in the ER. There, TGs are produced by diacylglycerol acyltransferases of the DGAT enzyme family (reviewed in Guo, et al., 2009). Sterols in contrast to TGs are transported into the cells via endocytosis and lysosomal degradation of lipoproteins. Like TGs, sterols can also be synthesized de novo in most cells (Guo et al., 2009).

Many different models exist concerning the actual formation of LDs. However, the actual LD biogenesis starts at the ER. The most accepted model suggests that neutral lipids accumulate between the membrane bilayer of the ER and form a “lens” that buds off eventually (Fig. 5, left panel, reviewed in Martin, et al., 2006). Another model, the so-called bicelle-model (Ploegh, 2007), claims that the neutral lipids between the ER membrane leaflets are excised from the membrane bilayer (Fig. 5, middle panel). The evolving LD

consists of cytosolic and luminal membrane parts of the ER phospholipid bilayer. A third model, the vesicular budding model, (Walther and Farese, 2008) starts with small bilayer vesicles that are bound to the ER membrane. Newly synthesized neutral lipids get pumped into the phospholipid bilayer of the vesicle filling up the space between the leaflets. Subsequently, the vesicle gets engulfed and forms an inclusion in the growing LD (Fig. 5, right panel).

LDs are complex and dynamic intracellular organelles. They communicate with other cellular organelles which is called heterotypic interaction. Those organelles that are involved in lipid metabolism were found to be in close apposition to LDs, like mitochondria (Sturmey, et al., 2006), ER (Turró, et al., 2006), and endosomes (Liu, et al., 2007). Furthermore, LDs can adapt to metabolic changes. In case of starvation, neutral lipids can be degraded by lipolysis and the FFAs processed by β -oxidation serve as energy source for the production of adenosine tri-phosphate (ATP). In contrast, if neutral lipids like TGs are in excess, additional storage space is required. As a result LDs have to grow. This issue has brought up some models that try to explain size increase of LDs.

In the first model it was shown by the authors of one study that an enzyme involved in long chain fatty acid synthesis, long-chain acyl-coenzyme A synthetase 3 (ACSL3), was abundantly associated with LDs in human hepatic carcinoma cell line (HuH7) (Fujimoto, et al., 2004). In the following study by this group this particular enzyme, ACSL3 was shown to contribute to local lipid synthesis at LDs by converting FFAs into free fatty acyl-CoA (Fujimoto, et al., 2007).

When the neutral core increases, the phospholipid monolayer has to grow too. This was shown to be accomplished by the enzyme CTP:phosphocholine cytidyltransferase (CCT) which was recruited to the LD surface in studies with *Drosophila melanogaster* (Guo, et al., 2008). Another model claims LD growth to be independent from TG biosynthesis by LD fusion. In this process LDs move along microtubules by means of the motor protein dynein (Boström, et al., 2005). Thereby the problem of utilizing or synthesizing additional phospholipids would not be required. In more detail, the fusion is dependent on a protein family called Soluble NSF Attachment Protein receptor (SNARE), responsible for vesicle fusion. Members of this family were found attached to LDs and knock out of certain SNAREs resulted in impaired droplet fusion (Boström, et al., 2007).

A variety of other proteins cover the LD surface permanently or temporally. They are either embedded in the membrane or attached to the monolayer by electrostatic or hydrophobic interactions. All of them contribute to the function of LDs. About 15% of them are members of the PAT protein family (Londos, et al., 1999) or lipid enzymes involved in lipid metabolism (Brasaemle, et al., 2004). In further studies in adipocytes it was shown that proteins from the

PAT family seem to be associated with LDs from the small emerging droplets at the ER until the mature LDs situated in the perinuclear area (Wolins et al., 2005).

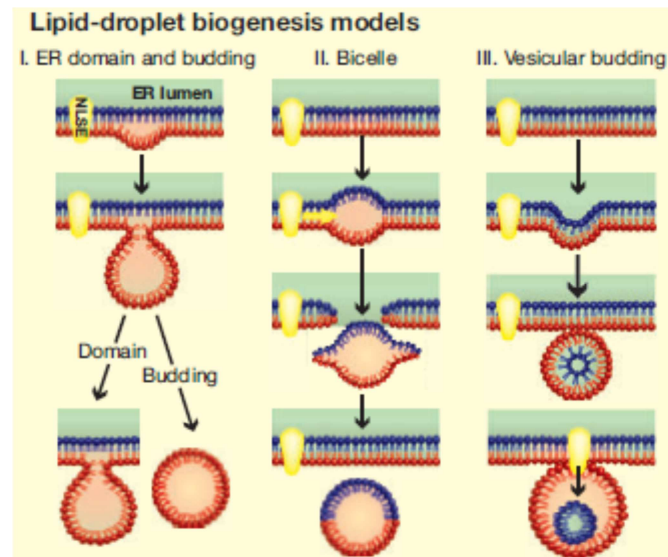


Figure 5. The process of LD evolution is depicted in this figure. Three different models were suggested. They are explained in detail in the text. The figure was taken from Guo et al., 2009.

1.4 PERILIPINS

PAT is the hypernym of a protein family also known as perilipins (PLINs). The name PAT stands for Perilipin (PLIN1), Adipose differentiation related protein (ADRP, ADFP, adipophilin, PLIN2), and Tail interacting protein47 (TIP47, PLIN3). This protein family was extended with two more recently found members called S3-12 (PLIN4), and OXPAT (LSDP5, PLIN5). For clarity throughout this thesis I will stick to the PLIN nomenclature as described above.

Despite the fact that it is not much known about PLIN proteins in the model organism chicken, the 5 members can be found in mammals as well as in evolutionary distant organisms like insects, slime molds, and fungi (Bickel, et al., 2009). All PLINs show distinct sequence similarities. An approximately 100 amino acid long stretch at the N-terminus, named PAT-domain, exists in all PLINs (except PLIN4) (Fig. 6). Additionally, an 11-mer region C-terminal to the PAT-domain was found in all mammalian PLINs. The similarity of PAT proteins in the 11-mer stretch does not concern the primary protein structure, indeed it was predicted that the secondary and tertiary structures do (reviewed in Bickel, et al., 2009).

Concerning the whole amino acid sequence, PLIN2 and PLIN3 share the highest sequence identity (43%). All PLINs have in common to be LD binding proteins, although a common binding domain for all PLINs has not been found to date. The 11-mer repeat was proposed to be a major factor for binding as it folds into α -helices with hydrophobic clefts being able to bind lipids in the cytosolic environment (reviewed in Bickel, et al., 2009). The PLIN proteins differ in tissue distribution, state of LD-binding, affinity to LDs, abundance when bound to LDs or in cytoplasm, and stability. One important feature that was suggested for all PLINs when bound to the LD membrane was to control access to the LD surface for other proteins (Wolins et al., 2003).

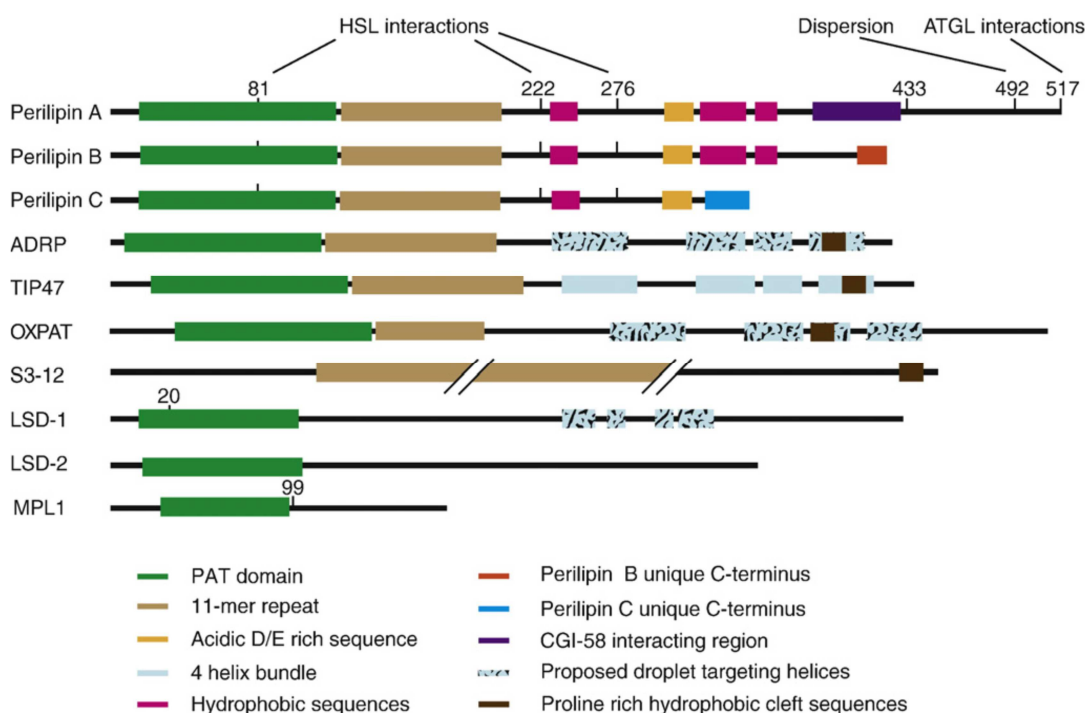


Figure 6. The figure shows sequence comparisons between PAT proteins. The first seven proteins are members of the mammalian PLINs. The last three (LSD-1, LSD-2, and MPL1) perform orthologous functions in flies and fungi. At the N-terminus all PAT proteins (except S3-12) show a high sequence similarity of about 100 amino acids, called PAT-domain. Additionally, the 11-mer repeats can be found in all mammalian PATs. The figure was taken from Bickel, et al., 2009.

1.4.1 PLIN1

In mice and humans PLIN1 is the most abundant PAT protein on adipocyte LDs of white and brown adipose tissue. Additionally, PLIN1 can be found at lower levels in steroidogenic cells.

The PLIN1 mRNA is spliced alternatively and gives rise to three isoforms. The PLIN1-A isoform is the most prominent one, found in adipocytes. PLIN1-B also exists in adipocytes but to a minor abundance. The third isoform, PLIN1-C is the least abundant and exists predominantly in steroidogenic cells (Servetnick et al., 1995). The vast majority of studies on PLIN1 focus on the isoform A. The PLIN1-A isoform has a size of approximately 60kDa in its non-modified state (Greenberg, et al., 1993).

As already mentioned, PLIN1 inhabits a PAT domain and an 11-mer repeat, both at the N-terminal part of the sequence (Fig. 6). A distinct feature of PLIN1 has been found in mutagenesis studies. Three hydrophobic sequence stretches in the central region of the PLIN1 amino acid sequence are required for LD targeting and the insertion of the emerging protein into the LD membrane (Subramanian, et al., 2004, Garcia, et al., 2003). PLIN1 is a constitutive LD-bound PAT protein also called CPAT (Bickel et al., 2009). It has a half-life of over 40h if associated with LDs (Brasaemle, 1997). It was found out that if PLIN1 detaches from the LD surface it gets quickly degraded by the proteasomal pathway (Xu, et al., 2006). A second feature distinct to all other PAT family members is the presence of 6 (mouse) protein kinase A (PKA) phosphorylation sites of serine residues. This kinase is cyclic adenosine monophosphate (cAMP) dependent (reviewed in Bickel, et al., 2009).

The PLIN1 protein functions and its activation of lipolysis in mammals are regulated as follows:

Under basal conditions (at non-lipolytic state) the LD bound PLIN1 hinders lipolytic enzymes to attach to the LD and thereby protects LDs from increased lipolysis. Additionally PLIN1 interacts with a protein called comparative gene identification 58 (CGI-58) that is recruited to LDs (Yamaguchi, et al., 2004). CGI-58, an α/β -hydrolase, in unbound state facilitates hydrolysis of cellular TG content (Brown, et al., 2007). A study by Martinez-Botas supports that assumption as follows. PLIN1 $-/-$ mice can consume more food compared to normal mice and still keep the same body weight. They are leaner and more muscular. Activity of an enzyme responsible for hydrolysis of stored neutral lipids, hormone sensitive lipase (HSL), was found to be highly increased compared to wild type mice. The adipocytes in white adipose tissue are about 62% smaller in size than in control organisms (Martinez-Botas et al., 2000).

PLIN1 gene expression is controlled by peroxisome proliferator-activated receptor gamma (PPAR γ) in adipocytes, which is induced hormonally by catecholamines like dopamine and norepinephrine (Fig. 7) (Arimura et al., 2004). The activation of this receptor has a strong effect on cAMP levels as signaling through G-proteins activates adenylyl cyclase. The cyclase then increases cAMP levels. The increased cAMP levels in turn activate cAMP dependent protein kinase A (PKA). The kinase poly-phosphorylates PLIN1 and HSL. PLIN1

detaches from the LD and HSL is thereby able to encounter the LD membrane (reviewed in Bickel, et al., 2009).

In the lipolytic status, when PLIN1 is phosphorylated, CGI-58 dissociates from PLIN1 and facilitates the LD binding of a second lipase called adipocyte triglyceride lipase (ATGL). ATGL mediates the first step of lipolysis from TGs to diglycerides (DGs). HSL cleaves off the second fatty acid to form monoacylglyceride. The final step performs a soluble monoglyceride lipase. Under basal conditions, ATGL and HSL are not able to encounter the LD properly and thereby no increased lipolysis occurs (reviewed in Bickel, et al., 2009).

A second receptor which activates PLIN1 expression was found to be the estrogen receptor-related receptor alpha (ERR α). The PPAR γ coactivator-1 alpha (PGC-1 α) itself activates ERR α (Akter et al., 2008).

Major properties of PLIN1 are summarized in table 1.

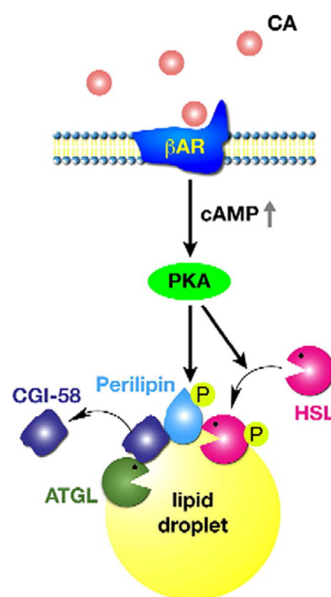


Figure 7. A model of the regulation of PLIN1 activity. Hormones like catecholamine activate β -adrenergic receptors and thereby increase cAMP levels. Then PKA is activated and phosphorylates PLIN1 which subsequently leads to the access of lipases like HSL and ATGL to the LD. The figure was taken from Bickel et al., 2009.

1.4.2 PLIN2

PLIN2 is a LD associated protein, which was first discovered by its high mRNA expression during adipocyte differentiation in the mouse (Jiang, et al., 1992). The sequence similarity to

the previously discovered PLIN1 led to further investigations and showed that PLIN2 coats small nascent LDs in various cell types (Brasaemle, et al., 1997). The human PLIN2 protein has a size of 50kDa and is constitutively bound to LDs (CPAT). PLIN2 proteins not associated with LDs get degraded by the ubiquitin/proteasome pathway (Xu, et al., 2005). A further modification of PLIN2 by phosphorylation may be possible as human phosphorylated PLIN2 (Serine 291) was detected via mass-spectrometry in HeLa cells (Bartz, et al., 2007). To date, no kinase has been discovered to phosphorylate PLIN2. A study by Nakamura and Fujimoto tried to find the LD-targeting domain of PLIN2. Many mutant fusion constructs of PLIN2 and enhanced green fluorescent protein (EGFP) with various truncations at the C- or the N-terminus were analyzed. Thereby it turned out that two non-overlapping sequences at both termini (aa 1–181 at the N-terminus, and aa 277–426 at the C-terminus) were sufficient for LD binding in mouse NIH3T3 fibroblasts. Additionally it was shown that both protein parts, fused to EGFP, were able to induce LD de-novo formation in rat PtK2 cells which have scarce endogenous LDs (Nakamura and Fujimoto, 2003).

PLIN2 expression is regulated by receptors of the PPAR-family. For example, PPAR- α activates PLIN2 in hepatocytes (Edvardsson, et al., 2006) and PPAR- β/δ in keratinocytes (Schmuth, et al., 2004). It was proven that PLIN2 expression, activated by PPARs, was stimulated by long-chain fatty acids in adipocyte precursor cells (Gao, et al., 2000).

In PLIN1 adipocyte knock out cells, PLIN2 coats LDs. However it cannot compensate functionally for PLIN1, as PLIN1 knock out leads to enhanced basal lipolysis (mentioned already in PLIN1 part). PLIN2 is abundantly expressed in almost all tissues except mature adipocytes, whereas PLIN1 seems to outcompete PLIN2 concerning LD binding. In non-adipocytes PLIN2 levels correspond with intracellular neutral lipids. Additionally, it was shown that LD formation increases concurrent with PLIN2 protein levels as new LD surface originates (reviewed in Bickel, et al., 2009).

PLIN2 was also found in in-vivo studies in mice to be involved in promotion of atherosclerosis. PLIN2 facilitated foam cell formation of macrophages induced by modified lipoproteins. Apolipoprotein E (apoE) knockout mice (apoE^{-/-}) have a high susceptibility to develop severe atherosclerosis (Paul, et Al., 2008). Deficiency of PLIN2 expression in the apoE^{-/-} background reduced the number of LDs in foam cells. An association between reduced numbers of atherosclerotic lesions and PLIN2 deficiency, and subsequent protection of these mice from atherosclerosis was additionally claimed by the authors (Paul, et Al., 2008).

A recent study by Chang et al., 2010, observed the changes in lipid metabolism on mRNA, protein, and lipid substrate levels between PLIN2-deficient obese mice and obese mice with intact PLIN2 expression. To accomplish this study, an obese mouse model of type-2 diabetes and non-alcoholic fatty liver disease (NAFLD) was used. Obesity was induced by gene knock out of the leptin gene ($Lep^{ob/ob}$), which causes the loss of feeling of satiety and thereby hyperphagia. Normally, leptin acts as a protein hormone secreted from the adipose tissue that regulates energy intake, energy expenditure, and appetite (reviewed in Chang et al., 2010).

PLIN2 deficient obese mice ($Lep^{ob/ob} / PLIN2^{-/-}$) compared to control mice ($Lep^{ob/ob} / PLIN2^{+/+}$) showed decreased plasma glucose levels after 4h fasting even though obesity was not ameliorated. Hepatocytes of $Lep^{ob/ob} / PLIN2^{+/+}$ mice showed a high amount of LDs filling up the whole cytoplasm, whereas in 50% of $Lep^{ob/ob} / PLIN2^{-/-}$ hepatocytes, LDs were bigger in size but more scarce in their number compared to control mice. The rest contained even fewer and smaller LDs. Total TG content in the liver was found to be approximately 25% reduced in PLIN2 deficient mice compared to control mice (Chang, et al., 2010).

Furthermore it was shown that PLIN2 is also involved in the regulation of very-low density lipoprotein (VLDL) secretion from hepatocytes. VLDL functions as the transporter of TGs and CEs in the blood. In $Lep^{ob/ob} / PLIN2^{-/-}$ mice, VLDL-mediated TG secretion was significantly increased. Additionally, the expression of microsomal triglyceride transfer protein (MTTP), responsible for VLDL assembly and secretion, was strikingly increased (Chang, et al., 2010).

Additionally, a study by Chang, et al., 2006 showed that PLIN2 deficient mice had a markedly reduced TG mass in their livers by 60% and also increased MTTP protein levels.

Similar results were found in a rat hepatoma cell line as PLIN2 overexpression increased TG accumulation and likewise decreased VLDL secretion (Magnusson, et al., 2006). Moreover, knockdown of PLIN2 by short interfering RNAs (siRNAs) reduced the storage of neutral lipids in LDs by 1/3, increased apolipoprotein B-48 (apoB)-48 expression 3.1-fold and induced β -oxidation (Magnusson, et al., 2006).

The findings of all those studies showed that PLIN2 has a strong ability to retain lipolysis. It promotes neutral lipid storage, LD formation, and regulation of LD size.

Major properties of PLIN2 are summarized in table 1.

1.4.3 PLIN3

PLIN3 is the third member of the PAT protein family. The protein gained its original name, TIP47, as it was found to bind to a phenylalanine/tryptophane motif in the “tail” of cytoplasmic cation-dependent mannose 6-phosphate receptor (MPR). TIP47 mediates the recycling of MPR from endosomal compartments to the trans-Golgi network (Díaz, et al., 1998). It is a 47kDa polypeptide whose relation to the PAT protein family was discovered due to its sequence similarities at its N-terminus, the PAT domain. Like PLIN1 and PLIN2, PLIN3 also contains an 11-mer repeat at its N-terminus.

PLIN3, like PLIN2 is expressed in almost all tissues and shares a high sequence similarity with it. Unlike PLIN2, PLIN3 is stable in the cytosol (about 6h) and is not rapidly degraded (Wolins, et al., 2001). The ability to bind LDs was first discovered in microscopy experiments in HeLa cells (immortalized human cervical cancer cell line). Addition of oleic acid to the cell culture medium strongly increased the LD association of PLIN3. In mouse MA10 Leydig cell homogenates, PLIN3 was mainly represented in the cytosolic fraction under lipid poor conditions. After lipid loading, PLIN3 was clearly redistributed from the cytosolic fraction to the lipid fraction (Wolins, et al., 2001). However, other studies could not confirm PLIN3 to be a lipid droplet associated protein (Barbero et al., 2001). More studies have to be done on PLIN3 to accurately tell its involvement in lipid metabolism.

The elucidation of the PLIN3 crystal structure revealed a four-helix bundle domain and an α/β domain with a hydrophobic cleft between them. The hydrophobic cleft was assumed to form a binding pocket (Hickenbottom, et al., 2004). Additionally it was discovered that apoE harbors a very similar four-helix bundle motif. The C-terminal part of apoE was predicted to create the driving force for protein:lipid binding (Saito, et al., 2001). The four helices of apoE were shown to bundle together in solution providing stability. As apoE is important in TG catabolism and therefore interacts with lipids, the same properties were assumed for PLIN3. Furthermore in a different study this hydrophobic cleft was predicted to be of great importance for recruitment of PLIN3 to the LDs (Ohsaki, et al., 2006).

A PLIN3 study showed that it can compensate for PLIN2 in mouse embryonic fibroblasts (MEFs) when PLIN2 is knocked out (Sztalryd, et al., 2006). After oleic acid administration, LDs formation was unaffected, and no differences were observed by means of lipid storage and lipolysis. Furthermore, PLIN3 mRNA knockdown with specific short interfering RNAs (siRNAs) resulted in decreased LD formation compared to the control group. Instead of TGs, phospholipids were the predominant stored neutral lipid species. Thereby they showed that the exchangeable LD binding protein (EPAT) PLIN3 is able to maintain normal LD formation and lipolysis in non-adipocytes.

Major properties of PLIN3 are summarized in table 1.

1.4.4 PLIN4

PLIN4 is a PAT protein which has been discovered much more recently than the first three ones. It was discovered in an antibody based screen for cell surface associated proteins involved in 3T3-L1 adipocyte differentiation (Scherer, et al., 1998). The PLIN4 gene expression is like PLIN1, and PLIN2 regulated by the hormonally stimulated PPAR γ receptor (Dalen, et al., 2004). It is the only PAT protein that inhabits no PAT domain. Nevertheless at the N-terminus of the 160kDa protein an extended 11-mer repeat has been detected which engages almost two thirds of the whole protein (Bussel et al., 2003).

PLIN4 was found to be involved mostly in fat storage activities. PLIN4 is predominantly expressed in white adipose tissue and to a lesser extent in skeletal muscle (Wolins, et al., 2003).

Furthermore it was shown that PLIN4 is stable in the cytosol under low lipid abundance and is therefore termed as EPAT, a not permanently LD-bound protein. After lipid loading, PLIN4 moves to the surface of LDs (Wolins et al., 2003). Additionally it was proposed that PLIN4 associates with growing LDs and thereby participates in LD biogenesis. In this particular study, the authors claim the finding that PLIN4 associates with small nascent LDs in the cell periphery after oleate supplementation in 3T3-L1 adipocytes. In lipid poor medium no PLIN4-coated LDs were detected. After lipid loading, next to the bigger perinuclear PLIN1-coated LDs, a small PLIN4-coated subpopulation of LDs was discovered (Wolins et al., 2003). However, more studies have to be done to elucidate all functions of PLIN4 and its relation to lipid metabolism.

Major properties of PLIN4 are summarized in table 1.

1.4.5 PLIN5

PLIN5 is one of the most recently discovered PAT proteins. Like PLIN3 and PLIN4, this protein is an EPAT, an exchangeable LD-binding protein. Its gene is situated on mouse chromosome 17 and human chromosome 19, in close proximity to the PLIN4 gene (Dalen et al., 2007). Although the PLIN5 gene is situated close to the PLIN4 gene, the proteins exhibit completely contrary functions. The PLIN5 gene is transcriptionally regulated by a member of the PPAR receptor family, PPAR α (Wolins, et al., 2006). PLIN5 is mainly expressed in heart, liver, brown adipose tissue, and skeletal muscle. Expression in those kinds of tissues points

out a specific function towards regulating the mobilization of energy depots, most likely in form of fat oxidation. PLIN5 mRNA translation gives rise to a protein of a size of approximately 54 kDa (Dalen, et al., 2007).

In microscopy studies a fusion construct with PLIN5 and a fluorescent tag was transfected into CHO-K1 cells. Under basal conditions (w/o oleate administration) the construct was visible throughout the cell. After the addition of oleate, LDs were formed and PLIN5 proteins were visible around those droplets. In human tissues it was shown that PLIN5 expression was induced after 12h of fasting conditions, especially in the liver (Dalen et al 2007). Concerning the liver, it was shown that PLIN5 expression was PPAR α dependent, whereas under fasting conditions PPAR α was not necessary for expression. Finally the investigations showed that PLIN5 exhibited protective functions against lipolysis under basal conditions compared to control cells (not expressing PLIN5) (Dalen et al., 2007).

A different study using Chinese hamster ovary cells (CHO) showed that PLIN5 is directly interacting with ATGL and thereby reducing lipolysis (Wang, et al., 2011). Mouse ATGL was tagged with a fluorescent protein and transfected into the cells. Interestingly, no direct interaction between PLIN1 and ATGL was found due to lacking presence of the co-factor CGI-58. No lipolysis by ATGL was observed in those cells when PLIN5 coated the LDs compared to control cells (no PLIN5). PLIN5 is thought to be of great importance concerning LD protection (anti-lipolytic) (Wang, et al., 2011).

Major properties of PLIN5 are summarized in table 1.

PAT protein	Regulated by phosphorylation	Promotes lipid storage	Recruits lipases or co-lipases	Role in intracellular trafficking	EPAT versus CPAT	PAT domains
PLIN1	Yes (PKA)	Yes	Yes	Yes (droplets)	CPAT	Yes
PLIN2	Unknown	Yes	Unknown	Yes (droplets)	CPAT	Yes
PLIN3	Unknown	Yes	Unknown	Yes (droplets)	EPAT	Yes
PLIN4	Unknown	Unknown	Unknown	Unknown	EPAT	No
PLIN5	Unknown	Yes	Yes	Unknown	EPAT	Yes

Table 1. Features of the 5 members of the PAT protein family in mammals. Table adapted from Bickel et al., 2009.

1.5 Lipases

The second aim of my master thesis was to identify enzymes, which could be responsible for the mobilization of the large TG depots in the YS. This process is called lipolysis and requires the action of lipid hydrolases, also called lipases. A necessary prerequisite for these enzymes is the affinity for TG substrates. TGs are the starting point for lipid degradation, as TGs (and CEs) are the predominant stored form of neutral lipids.

1.5.1 ATGL (Adipose triglyceride lipase)

This protein belongs to the Patatin like phospholipase (PNPLA) family. This investigated enzyme was named PNPLA2, ATGL, or desnutrin. It was first discovered in 2004, able to hydrolyze TGs to DGs and FFA but showed no affinity to other lipid substrates like CEs (Villena, et al., 2004). Hence, the enzyme was named adipose triglyceride lipase. The protein was shown to be most abundant during adipocyte differentiation. ATGL, like other members of this lipase family, contains a conserved patatin-like domain, common for plant acyl-hydrolases (Zimmermann, et al., 2004).

An interesting feature of ATGL is the response to feeding levels by increased/decreased mRNA expression. After fasting, ATGL expression was found to be highly increased. Additionally the mRNA expression is induced by glucocorticoids (Villena, et al., 2004). Insulin had the opposite effect as it decreased ATGL levels (Kershaw, et al., 2005).

A different study showed that beside adipose tissue, ATGL was found to be expressed in monkey kidney derived fibroblast cell lines (COS-7), and human cervical cancer cell lines (HeLa). In HeLa and Cos-7 cells, ATGL was found to localize to the LD surface after loading of oleic acid. Additionally it was discovered that ATGL is a main regulator of LD turnover (Smirnova, et al., 2006). Overexpression of ATGL resulted in a drastic decrease in LD size (1/50 compared to controls). Importantly, a mutation in the core of the catalytic domain of ATGL eradicated the LD-shrinkage phenotype. Thereby it was confirmed that ATGL is responsible for hydrolysis of TG depots stored in LDs (Smirnova, et al., 2006). ATGL has a co-factor that is important for its enzymatic function named CGI-58. In mouse studies the interaction between ATGL and CGI-58 showed a 20-fold increase in ATGL activity compared to the non-activated status. Furthermore, when CGI-58-gene carries point-mutations, the CGI-58 protein fails to activate ATGL. Mutant CGI-58 was found to be involved in Chananarin-Dorfman Syndrome (CDS), a disease caused by FFA-accumulation in the cytosol of many different tissues (Lass, et al., 2006).

1.5.2 PNPLA3 (Patatin-like phospholipase domain-containing protein)

A second member of the phospholipase family is PNPLA3, or adiponutrin. It was first found as a transmembrane protein whose mRNA was highly expressed during adipocyte differentiation (Baulande, et al., 2001). The PNPLA protein family descends from the patatin protein in potato tubers. Like mentioned for ATGL, PNPLA3 also inhabits a conserved N-terminal patatin-like domain which is mainly responsible for TG hydrolysis. Its catalytic center inhabits a serine-aspartate dyad (Rydel, et al., 2003; Jenkins, et al., 2004). In the study by Baulande, et al., 3 trans-membrane spans at the N-terminus were predicted by means of multiple sequence alignments (Baulande, et al., 2001).

A general model for PNPLA3 function was proposed by Pirazzi et al. FFAs are taken up into cells and esterified to neutral lipids (TGs) in the ER wherefrom they are stored in newly evolving LDs. PNPLA3 may encounter LDs to hydrolyze stored lipids and thereby produce again FFAs. Those FFAs then are redirected back to the ER and the Golgi where they are re-esterified into TGs. TGs then are transferred to apoB to assemble in nascent VLDL particles which then consequently are secreted (Fig. 8) (Pirazzi, et al., 2012).

Other important findings about PNPLA3 show a regulation of expression by feeding. A study with human cells (Huh-7) revealed that PNPLA3 expression is activated by the transcription factor sterol regulatory-element binding protein 1c (SREBP-1c). Additionally, SREBP-1c stimulated the transcription of genes involved in fatty acid biosynthesis. The accumulation of fatty acids increased the half-life of PNPLA3 in the cytosol and thereby promoted its stability (Huang, et al., 2010).

In the study by Kershaw, et al., which showed that ATGL expression levels were increased following starvation and decreased by re-feeding, PNPLA3 showed a complete opposite expression pattern. PNPLA3 mRNA was drastically decreased by starvation and showed elevated expression levels following re-feeding. Additionally, PNPLA3 showed an induction of gene expression by insulin, which again works the complete opposite to compared to ATGL (Kershaw, et al., 2005).

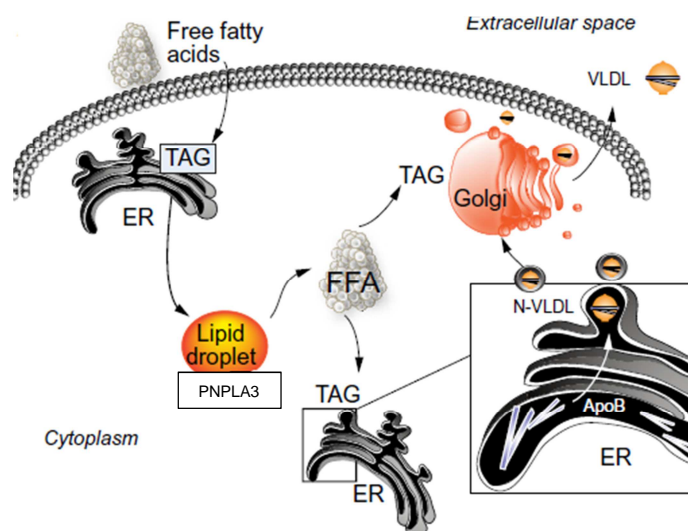


Figure 8. Proposed mode of action of PNPLA3. The figure was taken from Pirazzi, et al., 2012.

1.5.3 LAL (Lysosomal acid lipase)

Lysosomal acid lipase is an enzyme that is situated in intracellular compartments called lysosomes. It functions as a TG and CE lipase by breaking down CEs and TGs (Du, et al., 2008). LAL tissue distribution was tested in mice where it was shown to be expressed in almost all tissues. Highest expression levels were found in liver, adrenal gland, kidney, pancreas, and in the small intestine (Du, et al., 1996).

The exogenous neutral lipids are delivered into the cell and to the lysosomes via LDL. LDL binds to the cell-surface LDL receptor and enters the cell via endocytosis. Within the endosome, the lipid-laden LDL is transported to the lysosome where LDL and its lipid cargo get degraded. The released cholesterol is then further used in cellular membranes where it is re-esterified to CE by acyl-CoA:cholesterol acyltransferase. By the release of new cholesterol from previously hydrolyzed LDL particles within lysosomes, cell-own production of cholesterol is retained. When the LAL gene is mutated the lipid-laden LDL cannot be degraded (reviewed in Goldstein, et al., 1975).

In humans, mutations in the LAL gene were found to be responsible for at least two different phenotypes: The more severe form manifests in the Wolman disease (WD). WD has an early-onset phenotype which is normally lethal within the first few years of life. Affected patients suffer from massive storage of CEs and TGs in liver and small intestine. The less severe phenotype is called cholesterol ester storage disease (CESD). A strong increase in CE deposits in the intestines and hepatomegaly are the main phenotypic manifestations.

CESD affected people survive longer due to a residual activity of LAL (Aslanidis, et al., 1996). In a human LAL study it was discovered that one specific splice junction mutation at Exon 8 causes the CESD outcome and not WD. All other mutations detected could be found in both diseases (Anderson, et al., 1999). In a study by Goldstein, et al., 1975, in human fibroblasts from CESD patients it was shown that mainly the non-hydrolyzed exogenously derived neutral lipids in LDL were accumulated in the cytoplasm. Lipolysis of endogenously derived/produced lipids was not affected.

The severity of the WD and CESD was shown by Du, et al., 2001, where LAL knockout in mice caused TG and CE accumulation in spleen, liver and small intestine and subsequent swelling of liver and spleen (hepatosplenomegaly). Furthermore, the lack of hydrolysis of exogenously derived lipids caused a depletion of white adipose tissue (WAT) and brown adipose tissue (BAT) (Du, et al., 2001).

1.5.4 HTGL (Hepatic triglyceride lipase)

Hepatic triglyceride lipase is a TG lipase expressed mainly in the liver and is a member of the same superfamily of lipases like lipoprotein lipase (LPL) (Hide, et al., 1992). Unlike in mice, the synthesized protein in humans is bound to the hepatic endothelium after secretion. The human protein has a size of 64 to 69 kDa, which differs due to its glycosylation state (Datta, et al., 1988). The protein inhabits highly hydrophobic sequences for lipid and heparin binding at the C-terminus. The catalytic site resides at the N-terminus and is covered by a “lid” domain that is responsible for correct substrate binding. In the case of HTGL a higher affinity to phospholipids than to TGs was discovered (Dugi, et al., 1995). HTGL hydrolyses TGs in chylomicron (CM) remnants, intermediate density lipoprotein (IDL), and high density lipoprotein (HDL). It additionally hydrolyses phospholipids in HDL (reviewed in Santamarina-Fojo and Haudenschield, 2000).

1.5.5 LPL (Lipoprotein lipase)

LPL belongs to the same lipase superfamily as HTGL (Hide, et al., 1992). It is a TG lipase expressed in parenchymal cells of adipose tissue and muscle. The site of action of the membrane-bound glycosylated lipase is the vascular endothelium. The protein has a size of 55kDa and needs to dimerize for appropriate action. Folding into active homo-dimers is triggered by calcium (Zhang, et al., 2005). Activation of LPL requires an apolipoprotein, apoC-II (Kinnunen, et al., 1977). Like in HTGL the catalytic domain resides at the N-terminus

and the LD binding domain at the C-terminus. The “lid”-domain again covers the catalytic domain and ensures appropriate substrate binding (Dugi, et al., 1995).

In chicken studies it was shown that LPL is the rate-limiting enzyme in lipoprotein metabolism in adipose tissue. The enzyme hydrolyses TGs in lipoproteins like CMs and VLDL as absence of LPL caused triglyceridemia and reduced fat storage. Infusion of anti-LPL antibodies in broiler chicken resulted in a great reduction of abdominal fat storage (reviewed in Bensadoun, 1991; Sato, et al., 1999).

2. Materials and methods

2.1 Chemicals and Enzymes

Chemicals for buffers, solutions and media were used from Calbiochem, PeqLab, Roth, Sigma-Aldrich, Gibco, Applichem, Merck, USB, VWR-Prolabo, FLuka, Thermo Scientific, Iwaki, Biorad, Difco, Qiagen, MRC, and Promega.

Polymerases: High Fidelity PCR Enzyme Mix (5units/ μ l) by Fermentas;

Super Script II Reverse Transcriptase by Invitrogen;

T4 DNA Ligase (5units/ μ l) by Fermentas;

Restriction enzymes: EcoRI (10units/ μ l) by Fermentas.

2.2 Bacterial strains and vector systems

For the transformation of cloning vector with insert, following bacterial strain were used:

Strain	One Shot TOP10 Chemically Competent <i>E. coli</i>
Genotype	<i>F-mcrAD(mrr-hsdRMSmcrBC)f80lacZDM15DlacX74DeoRrecA1araD139D(araIeu)7697galUgalKtpsL(StrR)endA1nupG</i>
Reference/ Source	Invitrogen

Table 2. Bacterial strain used for transformations.

For the amplification of inserts, following cloning vector was used:

Vector	pCR®2.1-TOPO®
Size	3,931 basepairs
Genotype	<i>LacZα</i> fragment, M13 reverse priming site, MCS, T7 promoter/priming site, M13 forward priming site, f1 origin, kanamycin resistance, ampicillin resistance, pUC origin
Reference/Source	Invitrogen, TA cloning kit

Table 3. Genotype of pCR 2.1-TOPO cloning vector

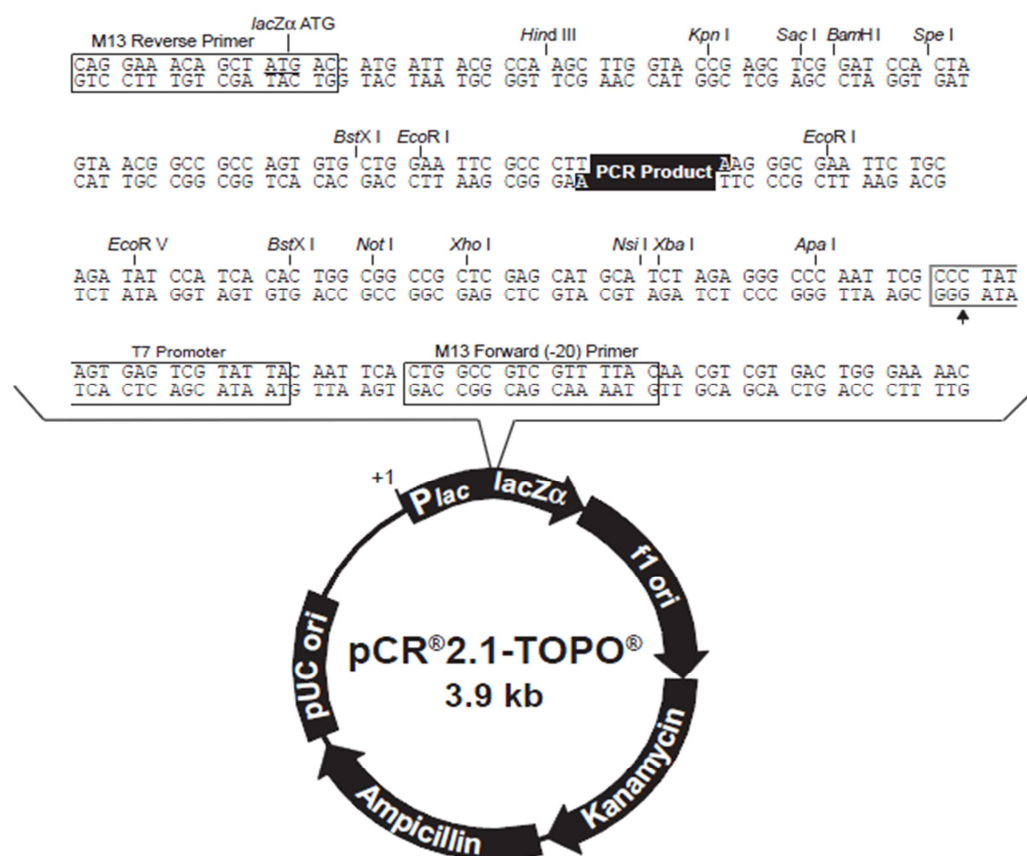


Figure 9. Genetic map of pCR 2.1-TOPO cloning vector

2.3 Oligonucleotide primers

Name	Sequence
PLIN1q-FWD	5'-GAGCCCCAGTTCTCAATGGC-3'
PLIN1q-REV	5'-GTCTCCACGGTGCTCTTGGT-3'
PLIN2q-FWD	5'-CCCACTGACAAGGTTGTTGCC-3'
PLIN2q-REV	5'-GCACCACACGACTTCCCAAG-3'
PLIN3q-FWD	5'-AGGCCCTTGGACAGCTTCAC-3'
PLIN3q-REV	5'-CAGGGACTCCATCTCCTCTGG-3'
PNPLA3q-FWD	5'-TGGCCAAAGAAGCTAGAAAGCG-3'
PNPLA3q-REV	5'-AAGCCTAGGAGGTAGACTCTC-3'
ATGLq-FWD	5'-AGCATCCAATTCAACCTTCG-3'
ATGLq-REV	5'-GAGAGGACCAGCAGGAC-3'
LALq-FWD	5'-AGCCCTCTGACAAAGCTGGG-3'
LALq-REV	5'-ACACGTCCACACGGCTCATA-3'
HTGLq-FWD	5'-GTGATCATTGCAGATTGGCTTAC-3'
HTGLq-REV	5'-TTTGTACCGCTGATGTA ACTACC-3'
LPLq-FWD	5'-CCATGGGTGGACGGTGACAG-3'
LPLq-REV	5'-GCAGCATGAGCACCCAGACT-3'

Table 4. Specific primers used for qPCR analysis

2.4 Animals

Mature Derco brown (TETRA-SL) laying hens were purchased from Diglas Co. (Feuersbrunn, Austria). Animals were kept cage free with free access to food and water. Light was provided for 14h per day. Fertilized eggs were provided by in-house chickens or from Schropfer GmbH, Schottwien, Austria. Eggs were sampled at embryonic day 0 and further incubated at 37°C for normal embryonic development. Chicken YSs were obtained from eggs 5days (d) post fertilisation.

2.5 Dissection of chicken yolk sac layers

First the egg was opened carefully with a scalpel. Then the whole egg-content was poured into a big petri dish. To start with the separation the embryo was cut off the YS and the yolk.

An important step was to completely remove the adhering yolk from the YS tissue. In the following step, the whole YS was transferred to a new petri dish filled with 1xPBS for washing. This step was repeated once. Now the different layers of the YS could be carefully separated. In the 5d embryo there was still a clear distinction between the vascularized (area vasculosa) and the non-vascularized tissue (area vitellina) of the YS. The white area vitellina at the periphery of the YS could be easily cut off from the vascularized layer with a scalpel. The vascularized tissue could be further separated into the blood vessel-containing layer (mesoderm and ectoderm) and the area beneath, the EECs from the area vasculosa. Finally, the different separated tissues could be weighed and aliquoted for further usage for RNA or protein-extractions.

2.6 Molecular biological methods: RNA

2.6.1 Total RNA extraction from chicken yolk sac tissue

Total RNA was isolated from tissue samples using TRIZOL reagent from MRC. Approximately 100mg of frozen tissue was weighed out into sterile microfuge tubes and placed on ice. 1ml of TRIZOL reagent was immediately added and vortexed shortly. The tissue in TRIZOL was transferred to a Potter homogenizer and homogenized, followed by 5 min incubation on ice. 0.2ml chloroform was added and the tube shaken vigorously for 15 sec. The tube was incubated on ice for 3 min, followed by a 15 min centrifugation step at 4°C at 12000xg. The aqueous phase containing the RNAs was taken off and transferred to a new tube. The RNA-phase was mixed with 0.5ml isopropanol and incubated at RT for 10 min. The sample was centrifuged at 12000xg for 10 min at 4°C. The supernatant was discarded and the whitish pellet was washed with 1ml 75% ethanol by centrifugation at 7500xg for 5 min at 4°C. The supernatant was discarded and the pellet dried for ca. 10 min at RT. It was of importance that the residual ethanol could evaporate but concurrently without drying the pellet completely which would have a negative effect on RNA concentration. According to the size of the pellet ddH₂O was added and the pellet dissolved at 60°C on a shaker. The dissolved RNA was frozen and stored at -80°C.

2.6.2 Reverse Transcription of isolated RNA

Reverse transcription of isolated RNA was performed with the Superscript II Reverse Transcriptase kit by Invitrogen. The RNA concentration measurement was done with a Nanodrop 2000c. Following components were mixed in a sterile microcentrifuge vial.

Oligo(dt) ₁₂₋₁₈ (500µg/ml)	1µl
Total RNA	1µg of total RNA
dNTP Mix (10mM)	1µl
ddH ₂ O	up to 12µl
Total	12µl

The mixture was incubated at 65°C for 5 min and then immediately chilled on ice.

The content of the tube was collected by brief centrifugation and following components were added to each reaction:

5x First Strand Buffer	4µl
0,1M DTT	2µl
Total	6µl

After incubation of the reaction mixtures for 2 min at 42°C, 1µl (200units) of Super Script II Reverse Transcriptase was added and the content mixed gently. The sample was incubated for 50 min at 42 °C. To inactivate the reaction samples were heated at 70°C for 15 min. Samples were centrifuged briefly and subsequently stored at -20°C or immediately used for amplification.

2.7 Molecular Biological Methods: DNA

2.7.1 Reverse transcriptase polymerase chain reaction (RT-PCR)

Polymerase chain reaction was used to amplify DNA sequences from previously synthesized cDNA. A thermocycler T3000 from Biometra was used. The total reaction volume of PCR experiments was 50µl. The polymerase used is listed in 2.1.

The following components were mixed in a nuclease-free microcentrifuge tube:

1µl cDNA
5µl 10x buffer (polymerase specific)
1µl forward primer (25pM/µl)
1µl reverse primer (25pM/µl)
1µl dNTP mix (10mM)
0.5µl polymerase
39.5µl ultrapure H₂O

Following PCR settings were used for primer pairs further used in real-time quantitative PCR (length up to 300bp; primer pairs are listed in table 4):

Procedure	Settings	
Initial denaturation	94°C for 5 min	
Denaturation	94°C for 30 sec	} 40x
Annealing	55°C for 30 sec	
Elongation	72°C for 30 sec	
Final elongation	72°C for 10 min	

The obtained PCR products were analysed by agarose gel electrophoresis.

2.7.2 Agarose gel-electrophoresis

The separation of DNA fragments was performed at a constant voltage of 100V for 30 min. Depending on the length of the fragment 1%, 1.5%, or 2% (w/v) agarose gels were used. The DNA samples were mixed with 5x DNA loading dye which contained Bromophenol blue or Xylene Cyanol FF used as front marker. Glycerol had a density increasing effect on the sample to ensure evenly loading into the sample well. To determine the size of the separated fragments the GeneRuler DNA ladder mix from Fermentas was used. To visualize the DNA bands under ultraviolet light (366nm) the fluorescent DNA-intercalating dye ethidium bromide was used.

50x TAE, pH 8.0

2 M Tris/HCl

1 M acetic acid

0.1 M EDTA

5x DNA loading buffer

50 % Glycerol

0.1M EDTA, 50x TAE Bromophenol blue or Xylen Cyanol FF

Ethidium bromide stock solution

10 mg/ml in ddH₂O

peqGOLD Universal Agarose by peqlab

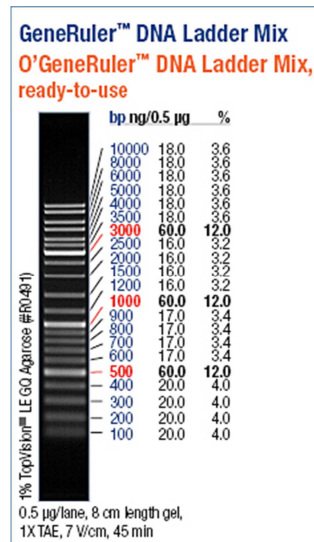


Figure 10. DNA Gene Ruler taken from <http://www.fermentas.com>

2.7.3 Agarose gel extraction

The gel extraction kit was provided by QIAGEN. This protocol was used to extract and purify DNA of 70bp to 10kb from standard or low-melt agarose gels in TAE or TBE buffer. All centrifugation steps were carried out in a tabletop centrifuge at the highest setting (13.000rpm). The desired DNA-fragment was excised from the agarose-gel with a sterile scalpel. 3 volumes of Buffer QG were added to the sample and incubated for 10 min at 50°C. To dissolve the gel properly, every 2-3 min the sample was vortexed. One volume of isopropanol was added and the sample transferred into a spin column (provided by QIAGEN). A centrifugation step for 1 min followed. The flow through was discarded and an additional centrifugation step was done with 0.5ml of buffer QG into the same collection tube. To wash the sample, 0.75ml Washing Buffer PE was added and after 5 min incubation the sample was centrifuged 1 min. The flow-through was discarded and another centrifugation step for 1 min was performed to drive off residual buffer. The column was now put into a new

sterile microfuge tube and 30µl of ddH₂O were added. After 1 min of incubation the purified DNA was eluted by a 1 min centrifugation step.

2.7.4 DNA ligation

To ligate the desired DNA fragment and a vector, a pCR 2.1 vector with the Invitrogen TA Cloning Kit was used. The DNA fragments were previously purified from an agarose gel like mentioned in 2.7.3. The vector and the fragment were first cut with the appropriate restriction enzyme. The ligation was carried out on ice and following components were mixed:

Gel-eluted PCR product	2µl
Ligation Buffer (10x)	1µl
pCR 2.1 vector	2µl
ddH ₂ O	4µl
T4-DNA ligase	1µl
Total	10µl

The sample was mixed by vortexing and short centrifugation. The incubation step was performed at 14°C overnight (O/N).

2.7.5 Production of chemical competent E. coli TOP10

Commercially bought TOP10 cells were inoculated in 5ml LB liquid medium and incubated O/N at 37°C on a shaker. 1ml of that O/N culture was inoculated into 200ml LB medium and shook at 37°C in 500ml flask to an OD of approximately 0,25 – 0,3. Then the culture was chilled on ice for 15 min. The 200ml culture was distributed to 4 50ml falcon tubes and centrifuged for 10 min at 3300xg at 4°C. The supernatant was discarded and the pellets dissolved in 20ml 0.1M CaCl₂ each. After 30 min incubation on ice the centrifugation (settings as above) was repeated and the pellets resuspended in 12ml 0.1M CaCl₂ solution + 15% glycerol. The cells were distributed into fresh sterile eppendorf tubes and frozen in liquid nitrogen. For long time storage they were transferred to a -80°C freezer.

2.7.6 Transformation of chemical competent *E. coli*

One aliquot (50µl) of chemical competent *E. coli* TOP10 cells were thawed on ice. Bacteria and plasmids were shortly centrifuged and placed on ice. 2µl of the TOPO TA ligation mixtures was added to one aliquot of competent cells. The cells in the vial were gently mixed and placed on ice for 30 min. Then the cells were heat shocked for 30 sec at 42°C and immediately returned on ice for 2 min. 250µl of room temperature (R/T) S.O.C. medium was added to the cells and regenerated for 1h at 37°C by shaking. 200µl of transformed cells were plated on LB-Amp (100µg/ml), LB-Kan (30µg/ml), or LB-Kan/X-Gal plates and incubated O/N at 37°C. Generally white colonies were expected. In case of X-Gal plates, white colonies indicated that the desired sequence was inserted into the X-Gal gene. The insertion into the X-Gal gene prevented expression and subsequent cleavage-induced blue staining. Liquid LB medium (with the suitable antibiotic) was inoculated with distinct white colonies to amplify the plasmids. The liquid culture was incubated at 37°C O/N on a shaker. To purify the plasmids from the bacterial culture a plasmid mini-preparation was performed.

2.7.7 Mini preparation of Plasmid DNA

Plasmid isolation was performed with the peqGOLD Plasmid Miniprep Kit I by PEQLAB. This plasmid preparation kit uses an alkaline lysis to degrade bacterial compounds and works completely without organic solvents. All centrifugation steps were performed in an Eppendorf Centrifuge 5418.

1ml of *E. coli* O/N culture was transferred to a sterile tube and centrifuged for 1 min at 10000xg. The supernatant was discarded and the previous step repeated. The cell pellet was dissolved in 250µl of solution I by vortexing. 250µl of solution II was added and mixed by gentle inverting of the tube. 350µl of solution III were added and again mixed gently by inverting the tube. The microfuge tube was centrifuged for 10 min at 10000xg. The liquid phase was transferred to the provided spin column to bind the plasmids to the silica-membrane without disturbing the white cell debris. The bound plasmids were washed with 500µl of PW plasmid buffer by 1 min centrifugation at 10000xg. 2 consecutive washing steps with each 750µl of DNA-wash buffer and 1 min centrifugation at 10000xg followed. To get rid of residual buffer and to dry the membrane, a 2 min centrifugation step at 10000xg was done. To elute the plasmids from the membrane, 50µl of ddH₂O were added, followed by a centrifugation step at 5000xg for 1 min. The purified plasmids were stored at -20°C.

2.7.8 Midi preparation of Plasmid DNA

For plasmid midi preparation the Pure Yield Plasmid Midiprep System by Promega was used. All centrifugation steps were performed in a Heraeus Sepatek Cryofuge 6000.

100ml of LB liquid medium containing the appropriate antibiotic was inoculated with 100µl of plasmid mini prep and incubated O/N at 37°C on a shaker. On the next day the O/N-culture was transferred to a falcon tube and centrifuged at 4000xg for 15 min. The supernatant was discarded and the pellet resuspended in 3ml Cell Resuspension Solution. 3ml Cell Lysis Solution was added and the lysate mixed by inverting the tube. The tube was incubated at RT for 3 min followed by the transfer of the lysate to the Pure Yield Clearing Column placed in a new, sterile falcon tube. The lysate was incubated at RT for 2 min and subsequently centrifuged for 5 min at 1500xg. The flow through was added to the Pure Yield Binding Column in a new, sterile falcon tube. A centrifugation step at 1500xg for 3 min followed. 5ml of Endotoxin Removal Solution was added and the column in the tube centrifuged for 3 min at 1500xg. Afterwards, 20ml of Column Wash Solution was added and centrifuged for 5 min at 1500xg. To remove residual ethanol, another centrifugation step was carried out for 10 min at 1500xg. The column was transferred to a new falcon tube, subsequently 500µl of ddH₂O were added and the plasmids eluted by centrifugation at 2000xg for 5 min into a sterile eppendorf tube. The purified plasmids were stored at -20°C.

Cell Resuspension Solution (CRA)

50mM Tris-HCl (pH 7.5)

10mM EDTA (pH 8.0)

100µg/ml RNase A

Cell Lysis Solution (CLA)

0.2M NaOH

1% SDS

Neutralization Solution (NSB)

4.09M guanidine

Hydrochloride (pH 4.2)

759mM potassium acetate

2.12M glacial acetic acid

Column Wash

162.8mM potassium acetate

22.6mM Tris-HCl (pH 7.5)

0.109mM EDTA (pH 8.0)

2.7.9 Restriction enzyme (RE) digestion

Following components were mixed and incubated for 90 min at 37°C:

10µl Mini/Midi prep

1µl appropriate RE

4µl appropriate restriction buffer

4µl ddH₂O

To investigate the degree of DNA fragment digestion, an agarose gel electrophoresis was performed. Positive Mini/Midi preps were sent for sequencing.

2.7.10 QPCR (Quantitative real time polymerase chain reaction)

QPCR (Quantitative Polymerase Chain Reaction) is an amplification method for nucleic acids (like common PCR) with the additional feature to quantify the amplified DNA.

SYBR Green was used for quantification via fluorescence measurement. It intercalates preferentially into double stranded DNA, and the resulting DNA-dye complex is able to absorb/emit light at 497nm and 520nm, respectively. Therefore, the fluorescent signal increases simultaneously with the amplified DNA. To ensure that only specific products of double stranded DNA are measured, a melting curve analysis is performed after the actual amplification program. Target double stranded DNA should melt at a specific temperature and the decrease of released fluorescent dye is detected. The melting curve of target DNA is different compared to unspecific by-products or primer dimers. This makes it possible to check the efficiency of the used primer pair and the quality of the obtained PCR product. Primer pairs which amplify additional unspecific products are not suitable for qPCR experiments.

To prevent primer-dimer formation the primers are specifically designed to not be able to bind each other.

qPCR Reaction Setup for Eppendorf Mastercycler:

PCR grade water:	8.2µl
KAPA SYBR Mastermix:	10µl
Forward primer (10µM):	0.4µl
Reverse primer (10µM):	0.4µl
Template DNA:	1µl
Total amount	20µl

Primers (100µM stock) and cDNAs were diluted 1:10 before used in the reaction setup.

Cycling Protocol:

Initial Denaturation / Enzyme activation:	3min 95°C	
Denaturation	3sec 95°C	} 40 x
Annealing	20sec 60°C	
Extension	8sec 72°C	

For each qPCR run triplicates for each tissue specific cDNA sample were used. Additionally a technical replicate of each of the triplicates was measured to recognize possible pipetting mistakes. Expression levels were measured in arbitrary units (AU).

2.8 Molecular Biological Methods: Protein

2.8.1 Protein Extraction: Whole TRITON X-100 tissue-extract preparation

One gram (g) freshly isolated or frozen tissue was transferred to a 15ml Falcon tube and placed on ice. 4ml of Homogenization Buffer was added and the tissue homogenized with an Ultra Turrax T25 homogenizer (Aigner), 3 times each 20 sec. The homogenate was centrifuged (SS34 rotor) at 620xg for 10 min at 4°C. The supernatant was transferred to an ultracentrifugation tube, and the detergent Triton X-100 (20% stock solution in ddH₂O) was added to a final concentration of 1%. The homogenate was incubated on ice for 30 min while

it was vortexed repeatedly. After a centrifugation step at 50000xg for 1h at 4°C, the supernatant was aliquoted and frozen at -80 °C.

Homogenization Buffer:

20 mM Hepes pH 7.4

300 mM Sucrose

150 mM NaCl

1x Proteinase inhibitor

2.8.2 Preparation of Triton X-100 membrane-protein extracts

All steps were performed on ice. One g of freshly obtained or frozen tissue was transferred to 15ml Falcon tube containing 5ml Buffer A. Proteinase inhibitor was added immediately to a 1x final concentration. The tissue was homogenized with an Ultra Turrax T25 homogenizer (Aigner) for 3 times each 20 sec. The homogenate was centrifuged for 10 min. at 3000xg at 4°C. The supernatant was then transferred to an ultracentrifuge tube and centrifuged at 4°C for 1h at 50000xg. The supernatant was discarded and the pellet resuspended in 1ml of Buffer A. Afterwards, the pellet was dispersed and homogenized using an 18 gauge needle and subsequently a 22 gauge needle. The homogenate was centrifuged for 1h at 4°C at 50000xg. The supernatant was discarded and the pellet diluted in Buffer B according to the size of the pellet (big pellet 2ml Buffer B). Then NaCl (4M stock solution) to a final concentration of 160mM was added. The homogenate was sonicated for 30 sec on ice. 26% ddH₂O of total volume was added followed by addition of 5% vol/vol TRITON X-100 to a final concentration of 1%. The homogenate was centrifuged for 1 h at 4°C at 50000xg, and the obtained supernatant was frozen at -80°C.

Buffer A: Buffer A: 20mM Tris/HCl, 1mM CaCl₂, 150mM NaCl; pH=8

Buffer B: 250mM Tris/HCl, 2mM CaCl₂; pH=6

2.8.3 Protein concentration measurement

For protein concentration measurement Bradford reagent by BioRad was used. First a standard curve with Quick Start Bovine Serum Albumin (BSA) standard as internal standard was established. 4 different concentrations were used: 4µg, 8µg, 16µg and 32µg BSA/ml Bradford reagent (Quick Start 1x Dye Reagent). Then 1µl of protein extract was added to 1ml

of Bradford reagent and mixed. The concentration was then measured with the absorption at 595nm wavelength.

SDS-PAA gel:

	Stacking Gel	10%	12%	14%
	4%			
dH2O	1525µl	2025µl	1675µl	745µl
1,5M Tris HCl pH 8,8	-	1250µl	1250µl	1250µl
0,5M Tris HCl pH 6,8	625µl	-	-	-
Bis-PAA	325µl	1650µl	2325µl	3255µl
10% SDS	25µl	50µl	50µl	50µl
10% APS	12.5µl	25µl	25µl	25µl
TEMED	5µl	5µl	5µl	5µl

Table 5. Electrophoresis procedure was performed in a BioRad Mini gel system in 1x SDS Running Buffer.

The gels were prepared with a thickness of 1mm. First the resolving gel was prepared by combining the components listed above in a 50ml Falcon tube. The mixture was transferred into the assembled gel system, overlaid with 1ml of isopropanol, and allowed to polymerize for ca. 20 min. After complete polymerization and the proper removal of isopropanol, the stacking gel with comb was poured on top of the resolving gel. The protein samples were mixed with 4xLaemmli buffer under reducing or non-reducing conditions. As a reducing agent, DTT was used at a final concentration of 25mM. Additionally, the reducing samples were boiled at 95°C for 5 min. The gel was run at 80 V until the Bromphenol Blue front reached the resolving gel and then shifted to approximately 150V until the Bromphenol Blue front ran completely out of the gel.

As a protein size marker, Unstained Precision Plus Protein Standard (Bio Rad) was used. On each gel 8µl of marker was loaded.

30% Polyacrylamide

29.2% acrylamide

0.8% N,N'-methylenebisacrylamide

4x Laemmli buffer

8ml 78% glycerol

6ml 20% SDS

0.4ml 1M Tris-HCl pH 7.4

ddH2O to a final volume of 20ml

+25mM Dithiothreitol (DTT) for reducing conditions

1x Electrophoresis buffer

25 mM Tris

0.192 M Glycine

1% SDS

2.8.4 Western blot analysis

Semi Dry Blotting

Proteins separated on the SDS-PAA gel were transferred to a nitrocellulose membrane (HybondTM-C Extra for optimized protein transfer, from Amersham Biosciences) by Western blotting in a semi dry blotting unit. The blot was built up as followed: Three Whatman papers soaked in 1x transfer buffer were superimposed on each other in the blotting unit, followed by the nitrocellulose membrane. On top of the membrane the SDS-PAA gel was put and overlaid with another three, 1x transfer buffer soaked Whatman papers. To remove air bubbles caught in between the layers, which would drastically reduce the quality of protein transfer, a test tube was rolled over the blot. The settings used for one gel were 200mA for 90 min. To visualize blotted proteins, the membrane was stained with Ponceau S staining solution for 2 min on a shaker.

Detection:

The membrane was blocked in 5% blocking solution (5% non-fat dry milk or 5% BSA) in 1xTBST for 1h on a shaker at R/T. Subsequently, the blocking solution was replaced by the primary antibody, which was diluted in blocking solution according to its affinity to the target epitope. The membrane was incubated with primary antibody O/N at 4°C on a shaker. After 3 washing steps, 10 min each with 1xTBST, the membrane was incubated with the appropriate secondary antibody (HRP-conjugated) diluted in blocking solution for at least 1h at RT on a shaker. Following 3 additional washing steps, the membrane was incubated with ECL solution I and II (ThermoScientific) mixed in a 1:1 ratio for 1min. Afterwards, the solution was removed carefully with tissue paper and the membrane placed in a developing cassette. After exposure times according to the signal intensity, films were developed in an Agfa Curix 60 developer.

2.8.5 Protein isolation from cellular lipid fractions by subcellular fractionation

Approximately 1-2g of area vitellina tissue was dissected from the chicken YS with a scalpel and adhering yolk was removed completely by washing the tissue extensively in 1xPBS. The tissue was centrifuged briefly to remove 1xPBS. Subsequently, the tissue then was mixed with 1ml lysis buffer containing 2M Sucrose. For homogenization the cells were incubated for 10 min on ice and vortexed every 2 min for 30 sec. After the addition of 3ml of lysis buffer and further incubation on ice for 10 min with periodical vortexing steps every 2 min, the now slightly viscous suspension was further homogenized by passing it a couple of times through a 27-gauge needle. To separate cell debris from cytosolic content 10 min centrifugation at 1500xg at 4°C followed. The supernatant was removed and transferred to a 12ml ultracentrifugation tube and subsequently overlaid with 2ml 0.27M sucrose in lysis buffer, 2ml 0.135M sucrose in lysis buffer and filled up to the top with lysis buffer. The tubes were sealed and centrifuged at 60000xg for 1h at 4°C. The lipid fraction floated up under the top of the tube while the cytosolic fraction was pelleted at the bottom. While the cytosolic fraction could be dissolved directly in 4xLaemmli buffer the lipid fraction was further processed by mixing with 5ml CHCl_3 : MeOH (2:1) and vortexing. The mixture was incubated on ice for 10 min followed by centrifugation at 1500xg for 10 min at 4°C. The proteins were visible as a white thin layer between the upper MeOH phase and the lower CHCl_3 phase. These adjacent phases were taken off with a syringe and a 27 gauge needle without disturbing the protein layer. The protein-phase was then mixed with 5ml diethyl ether : EtOH (3:1) by vortexing and incubated on ice for 10 min. Again, the samples were centrifuged at 1500xg for 10 min at 4°C. The precipitated proteins then were mixed with 5ml diethyl ether by vortexing. After 10 min incubation on ice and centrifugation performed as previously described, the white protein pellet was air-dried and subsequently dissolved with 4xLaemmli buffer.

Lysis buffer: 10mM Tris; 1mM EDTA; 1x protease inhibitor; pH=7.4

2.8.6 Subcellular fractionation method 2

Procedure adapted from Liu, et al., 2008

Purification of adiposomes: Approximately 1-2g of freshly obtained Area Vitellina tissue was placed into sterile 1.5ml eppendorf tubes. Excess liquid was removed from the tissue by centrifugation for 5 min at 500xg. Cells were resuspended in 4ml Buffer A by vortexing, followed by a 20 min incubation on ice. To homogenize the tissue, a Dounce-homogenizer (7ml capacity) was used. The pistil was pulled quickly out of the tube to break cell-

membranes by producing a depression. The homogenized cell suspension was incubated on ice for 15 min. To separate cell debris from cytosolic components, the samples were centrifuged at 4°C for 15 min at 1000xg. The supernatant was transferred to an ultracentrifuge tube with a 27 gauge needle. The tube with the cell lysate was overlaid and filled up with Buffer B. The sample was centrifuged for 1h at 4°C at 50000rpm. The floating lipid fraction was taken off with a pipette and transferred to a new eppendorf tube. The intermediate cytosolic fraction was transferred to an eppendorf tube and stored at -80°C for further processing. The pellet at the bottom of the tube which consisted of membrane debris was discarded. Excess buffer in the lipid fraction was separated from floating lipids by centrifugation at 4°C for 15 min at 10000rpm. Buffer was taken off with a tip, and care was taken not to disturb the floating lipids. This centrifugation step was repeated until almost no buffer was left. To remove membrane contaminations 1ml of Buffer B was added and subsequently the sample was centrifuged at 50000rpm for 10 min at 4°C. Floating lipids were transferred to a new eppendorf tube while residual buffer was discarded. The pellet at the bottom was resuspended in 200µl Buffer B and discarded. Remaining lipids attached to the tube were resuspended in 200µl Buffer B and pooled with the previously collected lipid fraction. The tube was centrifuged at 10000xg for 5 min at 4°C and the remaining buffer was taken off. Again the centrifugation step was repeated until no buffer was left. The lipid fraction was dissolved in an appropriate amount of 4xLaemmli buffer and used for Western blot analysis.

Buffer A: 20mM Tricine, 250mM Sucrose, pH=7.8

Buffer B: 20mM Hepes, 10mM KCl, 2mM MgCl₂, pH=7.4

2.8.7 Processing of the cytosolic protein fraction

1 volume of 100% TCA (trichloroacetic acid) was added to 4 volumes of cytosolic fraction-sample. The sample was mixed by vortexing and incubated on ice for 10 min. The sample was then centrifuged for 5 min at 14000rpm with a tabletop centrifuge. The supernatant was taken off very carefully without disturbing the protein pellet. 200µl ice cold acetone was used to wash the pellet. Another centrifugation step at 14000rpm for 5 min was performed. Acetone was added one more time followed by centrifugation with previous parameters. To dry the protein pellet, the sample was placed into a heat block and heated for 10 min at 95°C to evaporate residual acetone. Finally, the sample was mixed with the appropriate amount of 4x Laemmli buffer for further Western blot analysis.

2.9 Cultivation of EECs of the area vitellina

The freshly obtained area vitellina from 5d chicken YSs was collected and washed in 1xPBS as described in 2.5. Then the tissue was cut with a sterile scalpel. The tissue was cut into small pieces. These pieces were collected in a fresh Falcon tube and pelleted by centrifugation to remove PBS. Tissue pieces were resuspended in Dulbecco's Modified Eagle Medium F-12 (DMEM-F12) containing penicillin and streptomycin, glutamine and 10% fetal calf serum (FCS). The mixture was pipetted up and down to obtain a homogenous cell suspension. The cells were plated on 4-well Lab-Tek Permanok chamber slides and grown for at least 24h to confluence. Growth of cells was always monitored with a light microscope.

2.10 Immunofluorescence experiments

All fixations, incubations, washings and blocking steps were performed on a shaker. Washing steps were done in 1xPBS. Additionally, all incubation steps with fluorescent dyes and interspersed washing steps were performed in the dark.

Fixation of cells was performed in 4% paraformaldehyde in PBS for 20 min at R/T. Then, cells were washed 4 times at R/T for 5 min each in 1xPBS. Subsequently, cells were permeabilized and blocked for 45 min in 0.1% saponin, 3% BSA, and 0.2M glycine in 1xPBS at R/T. The incubation with the primary rabbit anti-human PLIN2 antibody was done O/N at 4°C in 0.1% saponin, 3% bovine serum albumin (BSA) in 1xPBS. Different antibody dilutions, from 1:100, 1:250, 1:500, to 1:1000 were tried to achieve the best epitope binding results. The next day, cells were washed three times, 5 min each at R/T in 1xPBS. Afterwards the cells were incubated with a Texas Red goat anti-rabbit secondary antibody for 1h diluted 1:500 in 1xPBS, followed by three washing steps, 5 min each at R/T. Nuclear staining was performed with 4',6-diamidino-2-phenylindole (DAPI) and LD staining with 4,4-difluoro-4-bora-3a,4a-diaza-s-indacene (BODIPY). Both fluorescent agents were diluted 1:500 in 1xPBS and incubated for 20 min. After the final staining the solutions were discarded and the slides dipped in ddH₂O. The slides were air dried in a light protected box and lastly covered with a few drops of DAKU fluorescent mounting medium and covered with a cover glass. The slides were then ready for microscopy or could be stored light protected at 4°C.

2.11 Utilized antibodies and antisera in Western blotting

Protein	Specific antibody	Dilution
huPLIN2	Rabbit anti-human PLIN2 antiserum	1:1000
Rabbit IgG	Goat anti-rabbit IgG	1:50000
ggLPL	Goat anti-chicken LPL antiserum	1:10000
Goat IgG	Rabbit anti goat-IgG	1:50000
ocGAPDH	Mouse anti-rabbit GAPDH antiserum	1:100000
Mouse IgG	Rabbit anti-mouse IgG	1:4000

Table 6. Used antibodies. All antibodies diluted in 5% milk powder, or 5% BSA in 1xTBST.

2.12 Utilized antibodies, antisera, and preimmune sera (PI) in immunofluorescence experiments

Protein/Preimmune serum	Specific antibody	Dilution
huPLIN2	Rabbit anti-human PLIN2 antiserum	1:100, 1:250; 1:500
Rabbit IgG	Goat anti-rabbit IgG	1:100, 1:250, 1:500
Rabbit preimmune serum	Rabbit preimmune serum	1:100; 1:250, 1:500

Table 7. Used antibodies and preimmune sera. All antibodies and PI diluted in 5% milk powder in TBST.

3. Results

The aim of my master thesis was to study and characterize LD associated proteins in the chicken YS. In particular I analyzed in detail the expression patterns of these special proteins in the chicken YS. I used quantitative PCR to study the expression on mRNA level and Western blotting and immunofluorescence to investigate protein abundance and intracellular localization respectively. In more detail I focused on proteins of the perilipin family, which have been shown to be LD associated. I could show that PLIN2 is the mainly expressed LD-associated protein in the chicken YS. After dissection of the YS into its distinct layers I found predominant expression of PLIN2 in the EECs of the area vitellina. As embryonic development proceeds, this tissue layer gets overgrown by the mesodermal blood vessel layer forming the fully differentiated area vasculosa. The area vitellina was formerly thought to be not involved in the nourishing process of the embryo, as there are no blood vessels to transport any components from those EECs. Instead, the area vitellina seems to be a “fat storing tissue” as I found PLIN2 in close association with LDs of its EECs, which occupy major parts of the cytoplasm (Fig. 2).

3.1 Investigation of PLIN gene expression in chicken tissues

Real time quantitative PCR was used to determine the relative expression levels of the perilipin gene family in chicken tissues. I investigated the expression patterns of PLIN1, PLIN2, and PLIN3. However, no chicken PLIN4 and PLIN5 sequences were found in NCBI and/or Ensembl database. PLIN1, PLIN2, and PLIN3 showed quite diverse results in expression levels and tissue distribution. In a first attempt I could show, as indicated in figure 11, that PLIN1 was highly expressed in adipose tissue (as expected and described in the introduction part) of adult animals but not in the 5d YS or adult laying hen liver tissue. In comparison, PLIN2 was expressed in all three tissues, the highest in liver tissue (Fig 12). PLIN3 showed an almost even, but low expression in all three tissues (Fig. 13).

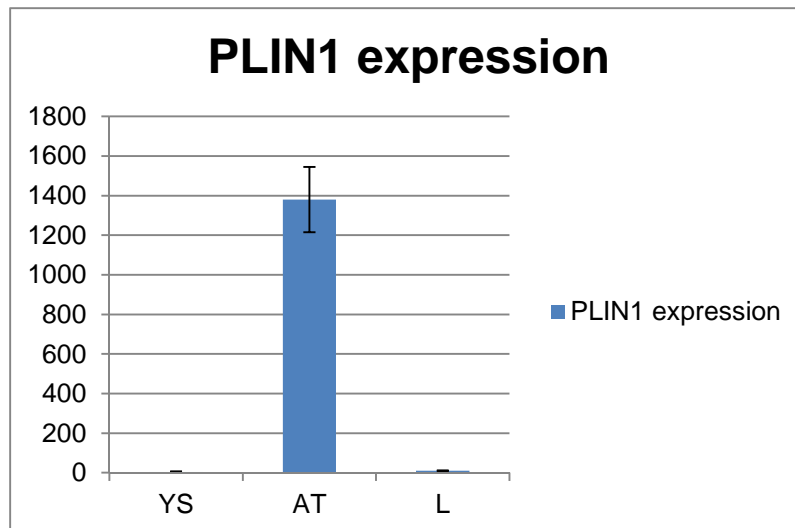


Figure 11. Levels of PLIN1 mRNA in YS, adipose tissue (AT), and liver (L). RNA was isolated from 5d chicken YS, adult laying hen AT and adult laying hen L tissue. QPCR experiments were performed after reverse transcription of total RNA as described in the Materials and Methods section 2.6.2. Transcript levels are expressed as arbitrary units (AU) and represent the average of at least triplicate measurements \pm standard error of the mean (S.E.M.).

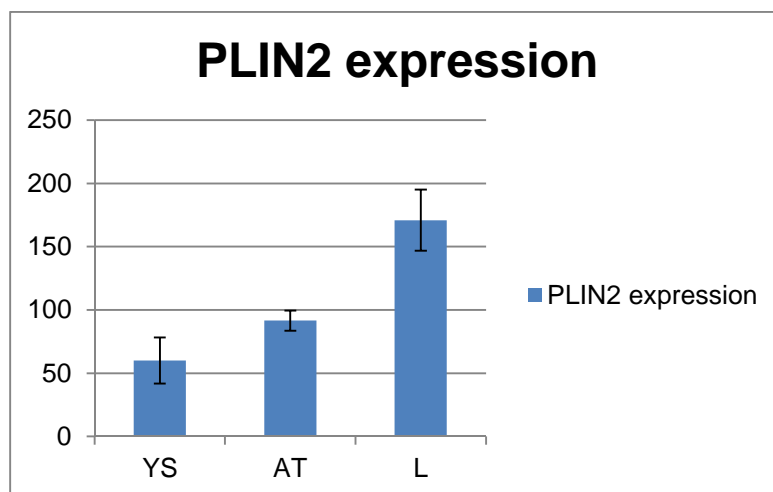


Figure 12. Levels of PLIN2 mRNA in YS, AT, and L. RNA was isolated from 5d chicken YS, adult laying hen AT and adult laying hen L tissue. QPCR experiments were performed after reverse transcription of total RNA as described in the Materials and Methods section 2.6.2. Transcript levels are expressed as arbitrary units (AU) and represent the average of at least triplicate measurements \pm S.E.M.

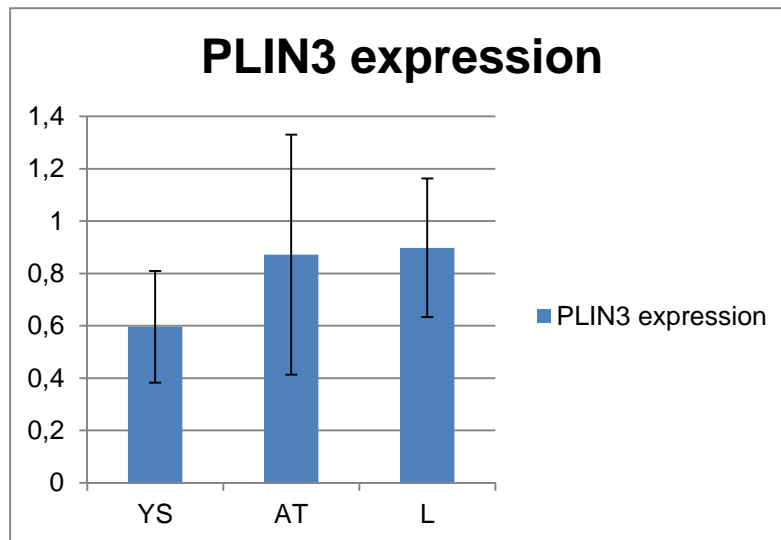


Figure 13. Levels of PLIN3 mRNA in YS, AT, and L. RNA was isolated from 5d chicken YS, adult laying hen AT and adult laying hen L tissue. QPCR experiments were performed after reverse transcription of total RNA as described in the Materials and Methods section 2.6.2. Transcript levels are expressed as arbitrary units (AU) and represent the average of at least triplicate measurements \pm S.E.M.

Next, I compared the expression levels of the three PLINs in the chicken YS 5d post fertilization. Interestingly, only PLIN2 was expressed at significant amounts compared to PLIN1 and PLIN3 (Fig. 14).

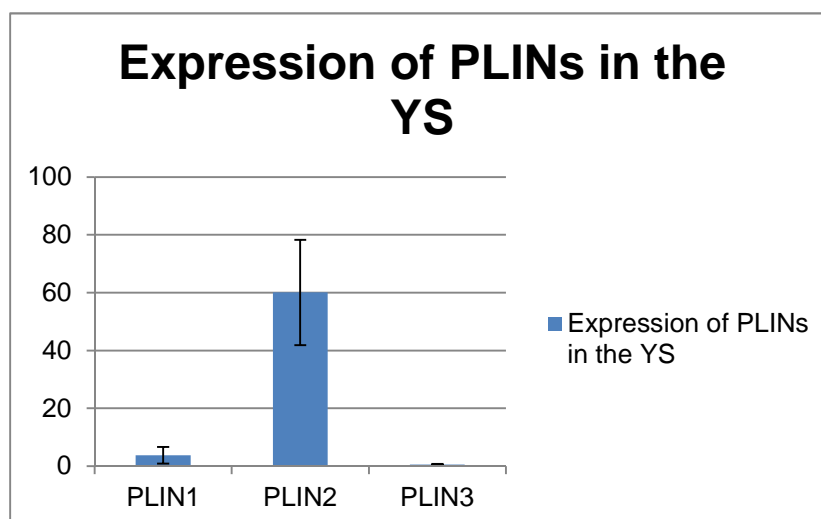


Figure 14. Levels of PLIN1, PLIN2, and PLIN3 mRNA in the chicken YS. RNA was isolated from 5d chicken YS tissue. QPCR experiments were performed after reverse transcription of total RNA as described in the Materials and Methods section 2.6.2. Transcript levels are

expressed as arbitrary units (AU) and represent the average of at least triplicate measurements \pm S.E.M.

To confirm those findings I dissected the 5d chicken YS into its distinct layers. First I performed qPCR with cDNAs, from EECs of the area vasculosa and from the mesodermal blood vessel layer. Again the same results were obtained (Fig. 15 and Fig. 16), and directed my focus towards the characterization of PLIN2 expression pattern and function in the chicken YS.

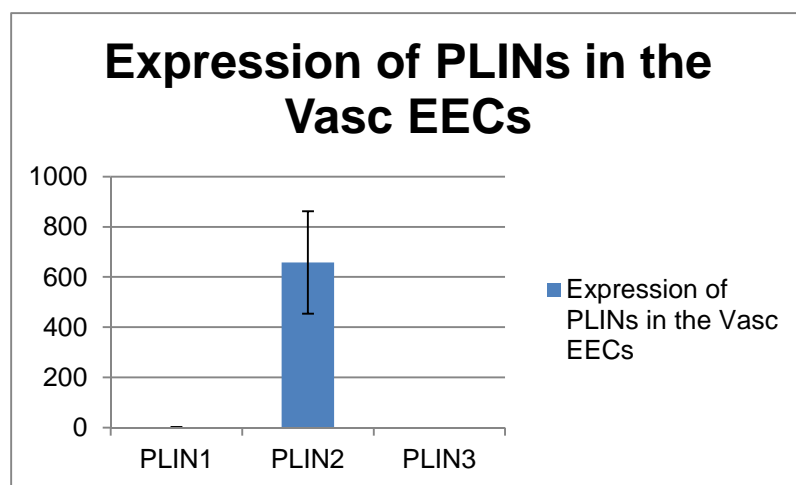


Figure 15. Levels of PLIN1, PLIN2, and PLIN3 mRNA in the EECs of the chicken YS. RNA was isolated from area vasculosa EECs of 5d chicken YS tissue. QPCR experiments were performed after reverse transcription of total RNA as described in the Materials and Methods section 2.6.2. Transcript levels are expressed as arbitrary units (AU) and represent the average of at least triplicate measurements \pm S.E.M.

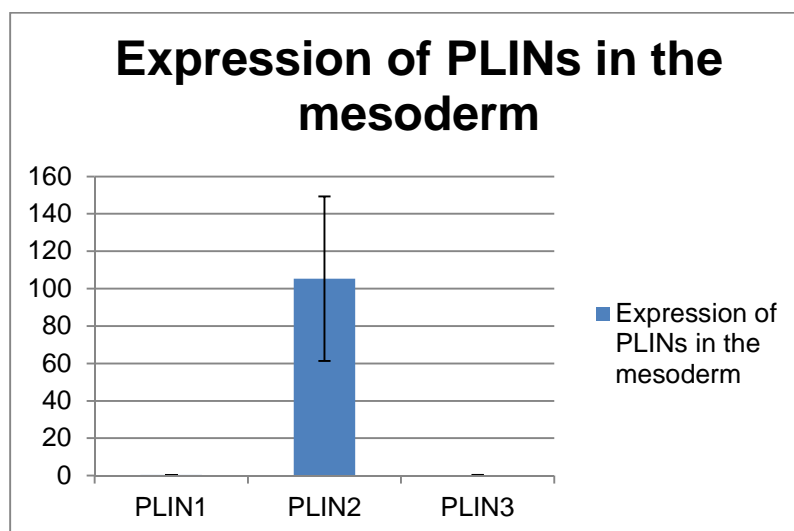


Figure 16. Levels of PLIN1, PLIN2, and PLIN3 mRNA in the mesodermal cell layer of the chicken YS. RNA was isolated from the mesodermal cell layer of 5d chicken YS tissue. QPCR experiments were performed after reverse transcription of total RNA as described in the Materials and Methods section 2.6.2. Transcript levels are expressed as arbitrary units (AU) and represent the average of at least triplicate measurements \pm S.E.M.

Furthermore, I compared the expression levels of PLIN2 in the EECs of the area vasculosa and in the blood vessel forming mesodermal cell layer (Fig. 17). PLIN2 expression in the EECs of the area vasculosa was approximately 6-fold higher than in the cells of the mesodermal layer.

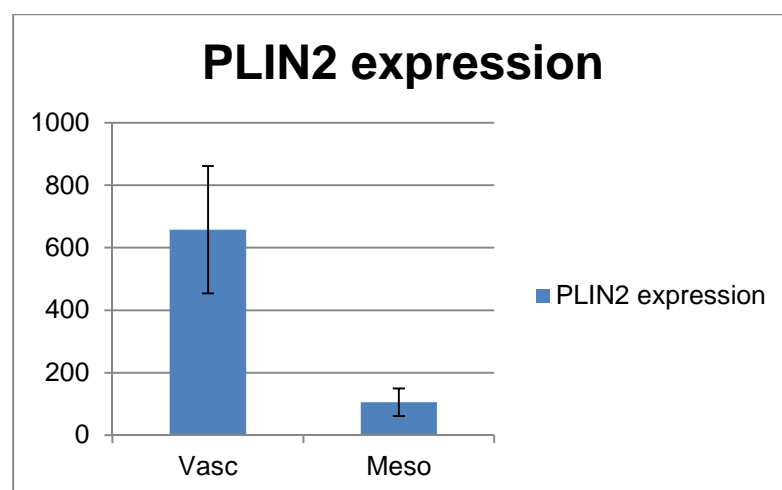


Figure 17. Levels of PLIN2 mRNA in the area vasculosa EECs and the mesodermal cell layer of the chicken YS. RNA was isolated from the area vasculosa EECs and mesodermal cell layer of 5d chicken YS tissue. QPCR experiments were performed after reverse transcription of total RNA as described in the Materials and Methods section 2.6.2. Transcript levels are expressed as arbitrary units (AU) and represent the average of at least triplicate measurements \pm S.E.M.

However, surprising results were obtained when qPCR experiments were done with all 3 cell sheets and the whole chicken YS (Fig. 18). The unvascularized EECs of the area vitellina showed a more than 100% higher PLIN2 expression than the area vasculosa EECs and the mesodermal cells. Those findings were later also confirmed on protein level.

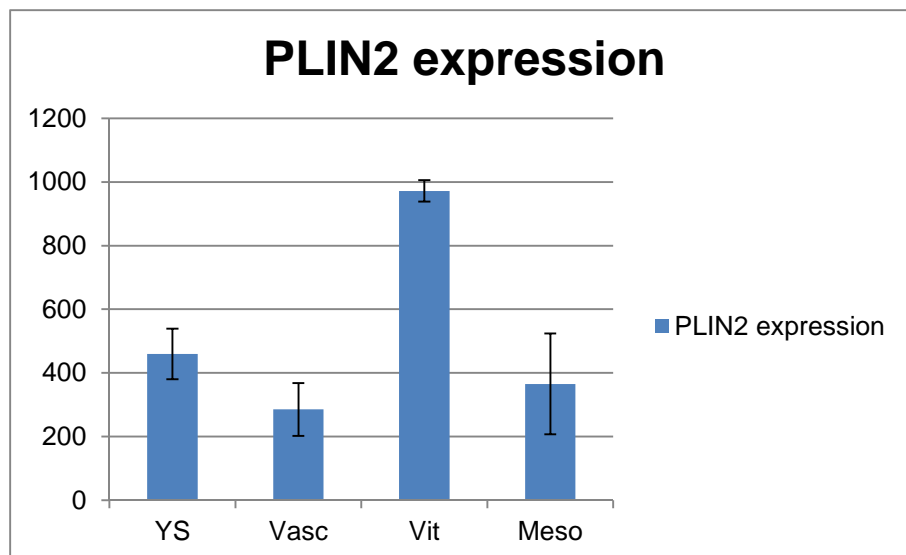


Figure 18. Levels of PLIN2 mRNA in the total YS, area vasculosa EECs, area vitellina EECs, and the mesodermal cell layer. RNA was isolated from 5d chicken YS tissue and its distinct cell layers. QPCR experiments were performed after reverse transcription of total RNA as described in the Materials and Methods section 2.6.2. Transcript levels are expressed as arbitrary units (AU) and represent the average of at least triplicate measurements \pm S.E.M.

3.2 Investigation of PLIN2 protein levels in the yolk sac.

Western Blots were performed to detect PLIN2 protein expression in the different cell layers of the chicken YS. It was of great interest if qPCR findings could be confirmed also on protein levels. First, as no specific anti chicken PLIN2 antibody was available in our lab, I had to search for commercially available antibodies with potential to crossreact with the chicken PLIN2 protein. Fortunately I found a rabbit polyclonal antibody directed against an epitope of human PLIN2, which shares great sequence homologies to the corresponding chicken PLIN2 peptide (provided by abcam) (Fig. 19).

gg Perilipin-2 MALAAIDPQQNIVSRVNLPLVSSTYDMVSTAYITTKDNHPYLKSVCEIAEKGVKTTITSV 60

hs Perilipin-2 MASVAVDPQPSVVTRVNLPLVSSTYDLMSAYLSTKDQYPYLKSVCEMAENGVKTTITSV 60

gg Perilipin-2 AMTSAMPPIIQKLEPQIVVANNYACIGLDKIEERLPILNQPTDKVVANAKGVVVGAREAVT 120

hs Perilipin-2 AMTSALPPIIQKLEPQIAVANTYACKGLDRIEERLPILNQPSTQIVANAKGAVTGAKDAVT 120

gg Perilipin-2	TTVSGAKETVAHKITGVVGKTKEAVQDSVEITKSVVNGGINTVLGSRVVQMMSSGMSAL 180
hs Perilipin-2	TTVTGAKDSVASTITGVMDKTKGAVTGSVEKTKSVVSGSINTVLGSRMMQLVSSGVENAL 180
	*****.*.*****:::*****:.*
gg Perilipin-2	TKSETLVDQYLPLTEAELEREAAKVEGFVGVQKPSYYVRLGSLSSKFRARAYQQALNKV 240
hs Perilipin-2	TKSELLVEQYLPLTEEELEKEAKKVEGFDL-VQKPSYYVRLGSLSTKLHSRAYQQALSRV 239
	**** *:***** **:** *****: *****:*****:*****:.*
gg Perilipin-2	RNAKQKSQETISQLHNTVSLIEYARKNMNSANQKLLGAQEKLQSWVEWKKNTGQNDGDE 300
hs Perilipin-2	KEAKQKSQQTISQLHSTVHLIEFARKNVYSANQKIQDAQDKLYLSWVEWKRSIGYDDTDE 299
	::*****:*
gg Perilipin-2	SHSAEHIESRTLAIASLTQQQLQTTCLTLVTSIQGLPQSVQDQVYSVRSMAGDVYEIFRS 360
hs Perilipin-2	SHCAEHIESRTLAIARNLTQQQLQTTCHTLLSNIQGVQPNIQDQAKHMGVMAGDIYSVFRN 359
gg Perilipin-2	ASSFQELSDSFLTTSKGQLKKMKESLDDVMDYLVNNTPLNWLVGPFYPQLPGTQHAENEG 420
hs Perilipin-2	AASFKEVSDSLTSSKGQLQKMKESLDDVMDYLVNNTPLNWLVGPFYPQLTESQNAQDQG 419
gg Perilipin-2	EGEKNSSQEDK----- 431
hs Perilipin-2	AEMDKSSQETQRSEHKTH 437



Figure 19. Alignment of chicken and human PLIN2 protein sequences. In red, the binding epitope of the rabbit anti-human PLIN2 antibody is indicated. Red asterisks indicate 100% homology of the amino acid sequence between the two species. The lower picture shows the position of the binding epitope of the PLIN2 antibody in the primary protein sequence, indicated in red.

As shown in figure 20, results from qPCR experiments were confirmed by the specific binding of rabbit anti-human PLIN2 antibody to a chicken protein with a molecular weight of approximately 48kDa in a total protein extract of 5d chicken YS containing area vasculosa and area vitellina tissue. No PLIN2 protein could be detected in the EECs of the area vasculosa (Va) and the mesodermal, blood vessel – containing cell layer (Me). However, a strong signal for PLIN2 was detected in the area vitellina (Vit), which perfectly matches the

observations from qPCR experiments. As a loading control, a monoclonal mouse anti-rabbit glyceraldehyde 3-phosphate dehydrogenase (GAPDH) antibody was used.

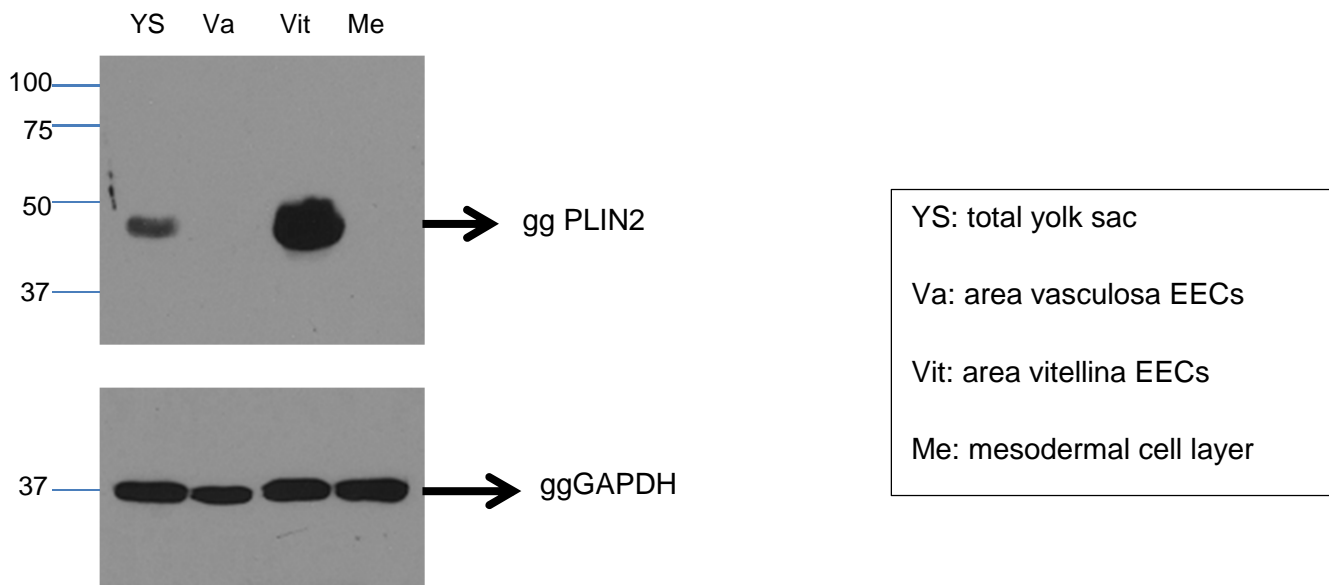


Figure 20. Top panel: Western blot under reducing conditions shows the presence of PLIN2 in total chicken YS and its individual cell sheets. 50µg of total protein extracts was loaded to a 12 % SDS-PAA gel followed by transfer to a nitrocellulose membrane. Chicken PLIN2 was detected with a crossreactive rabbit anti-human PLIN2 antibody. As secondary antibody, HRP-conjugated goat anti-rabbit IgG by Sigma Aldrich was used. To visualize specifically bound antibodies the enhanced chemiluminescent (ECL) system ECL was used. A molecular weight standard was used to determine the size of detected proteins in kDa.

Bottom panel: Western blot under reducing conditions shows the presence of GAPDH in total chicken YS and its individual layers. The antibody used was a mouse anti-rabbit GAPDH monoclonal antibody. As secondary antibody, a HRP-conjugated rabbit anti-mouse polyclonal antibody was used.

To determine the specific localization of PLIN2 in EECs of the area vitellina, I performed subcellular fractionation experiments as described in the Materials and Methods section (2.8.5, 2.8.6, and 2.8.7). Thereby I isolated the cell content from the cell membrane by using a lysis buffer. The lipid fraction was then separated from the cytosolic fraction by ultracentrifugation. Subsequently both fractions were processed separately to isolate the proteins. Eventually Western blots were performed.

As a control, area vitellina total protein extracts were used. PLIN2 protein seemed to be predominantly present in the lipid fraction of the area vitellina. On the blot, slight bands could be detected. No antibody staining was visible in the cytosolic fraction (Fig. 21).

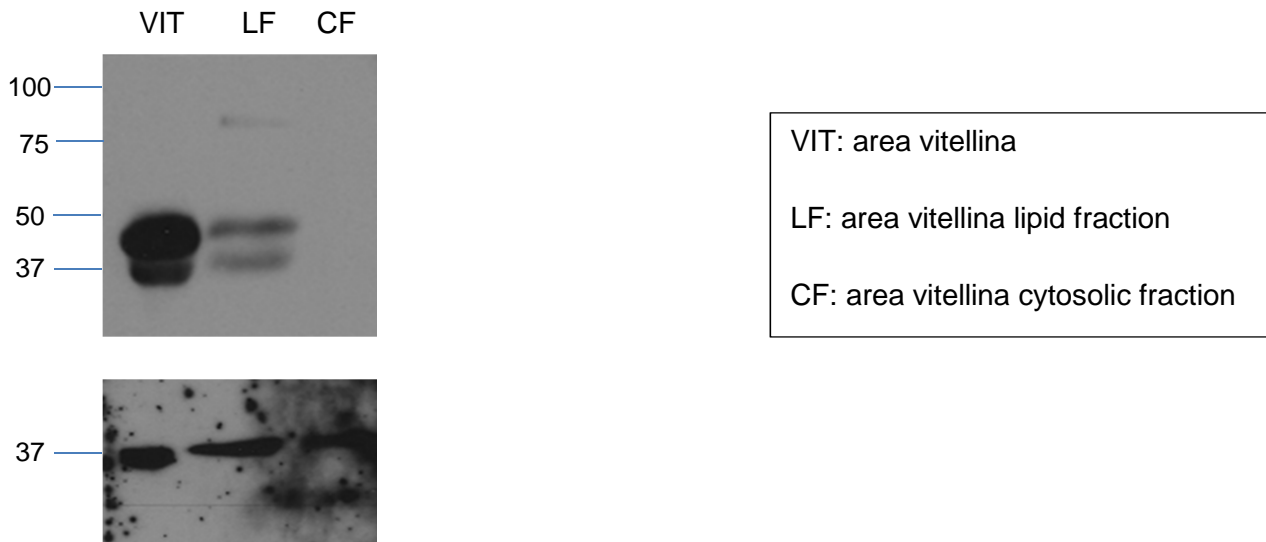


Figure 21. Top panel: Western blot under reducing conditions shows the presence of PLIN2 protein in subcellular fractions of the area vitellina. As a control and reference, area vitellina total protein extract was used. 50µg of total protein extract of each fraction was subjected to a 12 % SDS-PAA gel. The proteins were subsequently transferred to a nitrocellulose membrane. A rabbit anti-human PLIN2 polyclonal antibody was used. As secondary antibody, HRP-conjugated goat anti-rabbit IgG by Sigma Aldrich was used. Antibody binding was visualized with ECL solution. A molecular weight standard was used to determine the size of detected proteins in kDa.

Bottom panel: Western blot with the same cellular fractions as shown in the top panel. As a loading control, GAPDH was used and detected with a mouse anti-rabbit GAPDH monoclonal antibody. As secondary antibody, HRP-conjugated rabbit anti-mouse IgG was used.

3.3 Immunofluorescence: PLIN2 antibody staining in area vitellina EECs

To learn more about the detailed localization of PLIN2 in the cells of the area vitellina, I performed immunofluorescence stainings. Cells were stained with rabbit anti-human PLIN2 antibody and the binding was visualized with a Texas Red labeled goat anti-rabbit secondary antibody. A number of staining experiments were performed to optimize the protocol for

cultivation and antibody incubation (Fig. 22 and Fig. 23). As a control, and to confirm the specificity of the PLIN2 staining pattern, a preimmune serum (PI) (Fig. 24) was used to show unspecific staining. The weak greenish, blurry staining, which is visible throughout the majority of cells analyzed most likely occurred due to broken up LDs during the fixation and/or staining process.

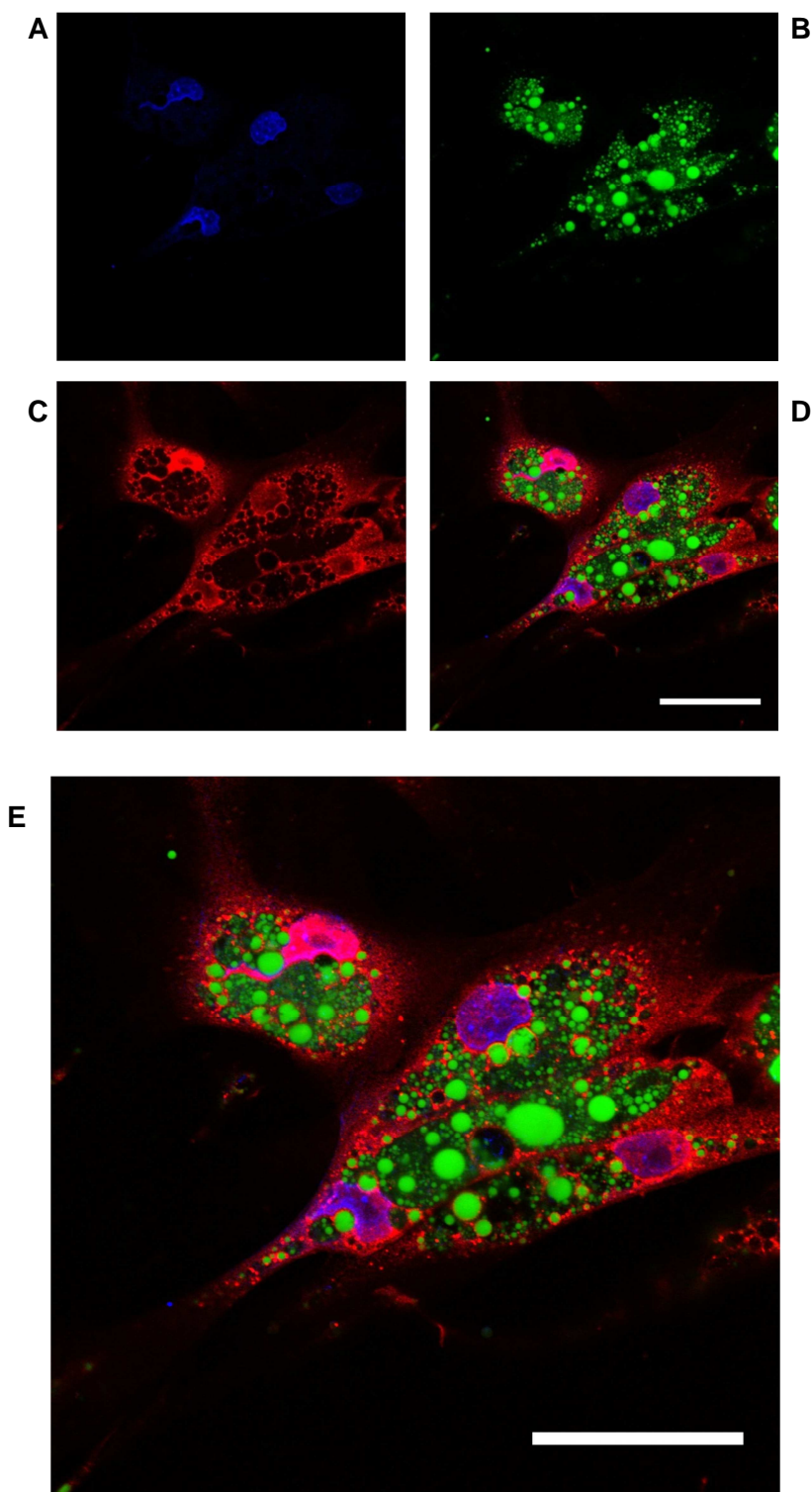
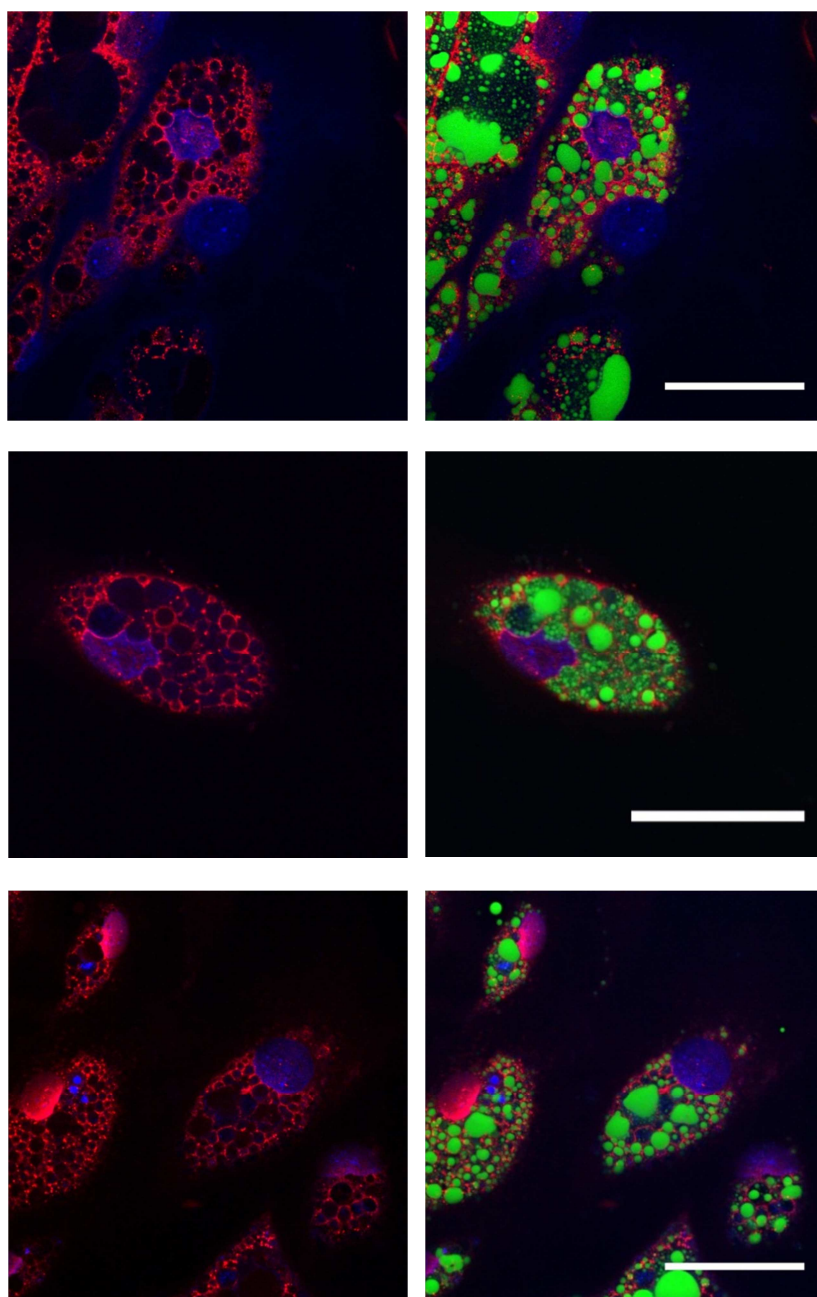


Figure 22. PLIN2 immunofluorescence stainings of cultivated area vitellina EECs from 5d chicken YS. Cells were grown for 48 h and subsequently fixed in 4% PFA and further processed as mentioned in the Materials and Methods section (2.10). Picture A shows nuclear staining with DAPI. Picture B shows LD staining with BODIPY, and in Picture C the specific staining of PLIN2 proteins with Texas Red goat anti-rabbit secondary antibody is depicted. Picture D and E show the merged picture. Images were taken with an LSM 510 confocal microscope using a 63x oil objective. Scale bar: 50µm.



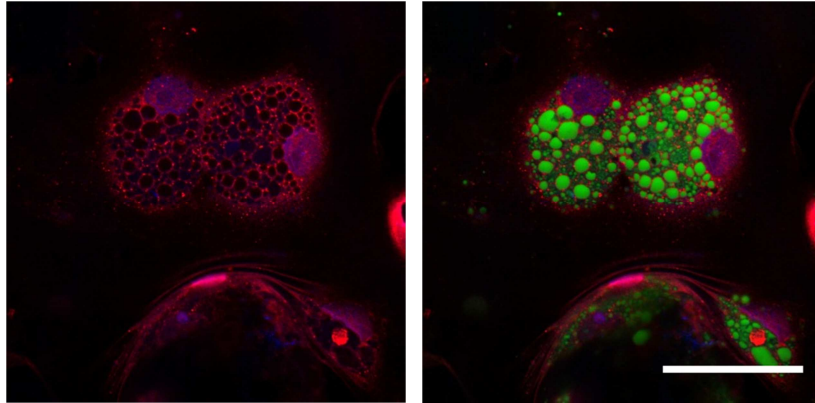
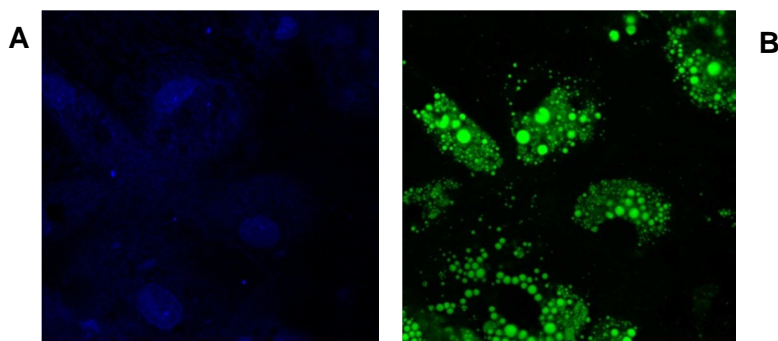


Figure 23. PLIN2 immunofluorescence stainings of cultivated area vitellina EECs from 5d chicken YS. Cells were grown for 48 h and subsequently fixed in 4% PFA and further processed like mentioned in the Materials and Methods section (2.10). PLIN2 protein localization was determined using a primary polyclonal rabbit anti-human PLIN2 antibody and a secondary Texas Red goat anti-rabbit antibody for visualization. LD staining was done with BODIPY (green). In blue the nuclear staining with DAPI is shown. Images on the left side show merged pictures of DAPI and antibody staining. Figures on the right show the merged picture of DAPI, antibody and BODIPY staining. The images were taken with a LSM 510 confocal microscope using a 63x oil objective. Scale bar: 50 μ m

3.4 Immunofluorescence: PI staining in area vitellina EECs

As control experiment, and to confirm specificity of the rabbit anti-human PLIN2 staining pattern, I used a rabbit pre immune serum (PI). As depicted in figure 24, and 25, a general unspecific background staining in red could be observed.



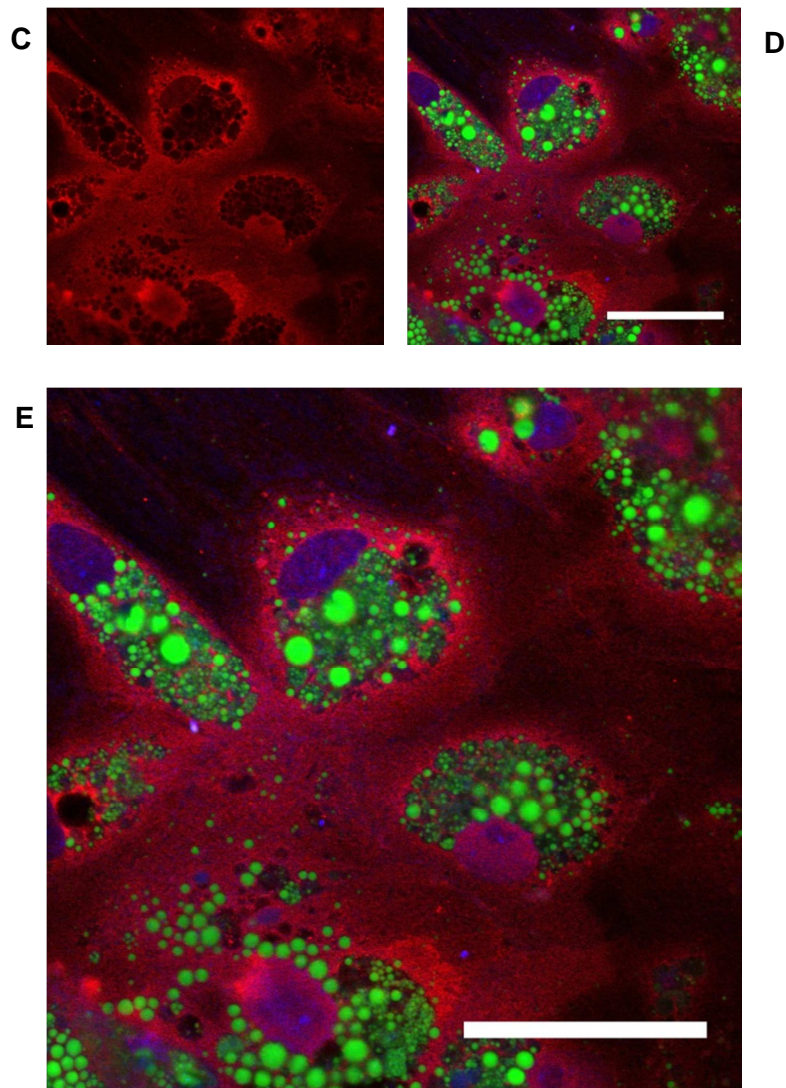


Figure 24. Preimmune staining of cultivated area vitellina EECs from 5d chicken YS. Cells were grown for 48 h and subsequently fixed in 4% PFA and further processed as mentioned in the Materials and Methods section (2.10). Picture A shows nuclear staining with DAPI, LD staining with BODIPY is depicted in picture B, and the PI staining visualized with a Texas Red goat anti-rabbit secondary antibody is shown in picture C. Picture D and E show the merged image. The images were taken with a LSM 510 confocal microscope, using a 63x oil objective. Scale bar: 50µm.

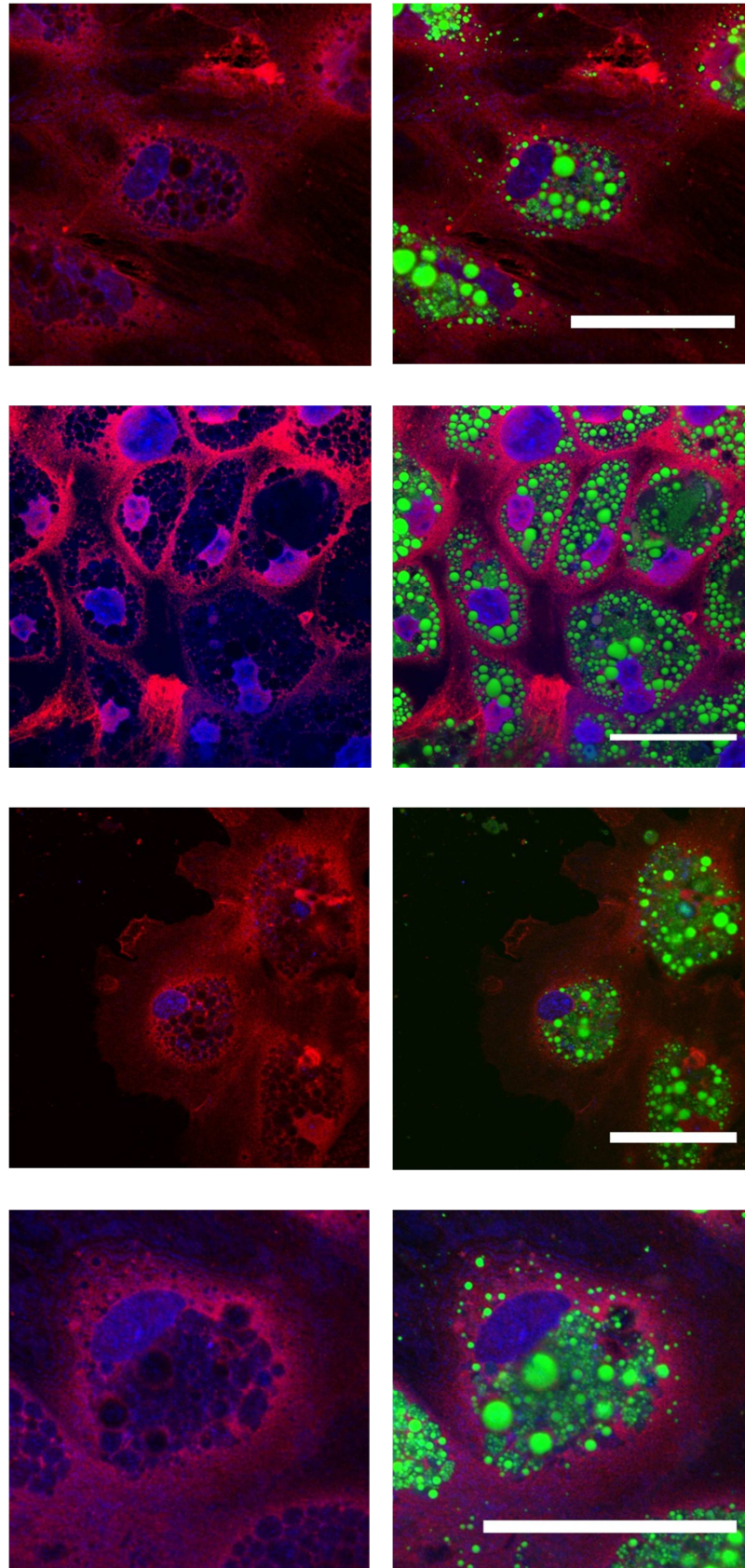


Figure 25. Preimmuno staining of cultivated area vitellina EECs from 5d chicken YS. Cells were grown for 48 h and subsequently fixed in 4% PFA and further processed like mentioned in the Materials and Methods section (2.10). A rabbit PI serum was used as unspecific

primary antibody. For visualization, again a Texas Red labeled goat anti-rabbit secondary antibody was used. LD staining was performed with BODIPY (green). In blue, the nuclear staining with DAPI is shown. Figures on the left side show merged pictures of DAPI and Texas Red staining of the PI. Figures on the right show the merged picture of DAPI, PI and BODIPY staining. The pictures were taken with a LSM 510 confocal microscope, using a 63x oil objective. Scale bar: 50µm.

To sum up, the here presented findings indicate an involvement of PLIN2 in the fat-storing regulation in the endodermal cells of the chicken YS. PLIN2 expression was clearly detectable on mRNA level (Fig. 18) as well as on protein level (Fig. 20). Additionally, the immunofluorescence investigations confirmed the results obtained by Western blotting by showing the clear association of PLIN2 with the lipid fraction of the cells (Fig. 21). Even though mRNA expression seems to be very weak for PLIN1 and PLIN3, further investigations have to be done on protein level. Unfortunately, due to lacking chicken sequences of PLIN4 and PLIN5, a potential participation of these gene products and/or proteins could not be investigated.

3.5 Lipases involved in the mobilization of TGs in the chicken yolk sac

The huge amounts of lipids stored in the EECs of the area vitellina eventually get involved in metabolic processes as the differentiation to the area vasculosa proceeds. ApoB containing TG-rich lipoproteins are assembled and secreted exclusively in the area vasculosa of the chicken YS (Bauer, et al., 2012, unpublished data). As lipoproteins are responsible for the transport of fats, TGs, stored in LDs, have to be mobilized from their compartments. Therefore, we speculated that specific TG hydrolyzing enzymes must be involved in the release of stored lipids during the transition from the area vitellina to the area vasculosa in the chicken YS. I tested various TG lipases to find the potential rate determining enzymes.

I performed qPCR experiments to determine expression levels of well-known lipases, generally involved in TG breakdown. First I tested ATGL, a rate determining enzyme concerning TG hydrolysis and mobilization from adipocyte LDs. In qPCR analysis it was shown that on the one hand ATGL mRNA was higher expressed in the area vasculosa compared to the undifferentiated EECs of the area vitellina but it seemed that highest

expression occurred in the mesodermal blood vessel layer (Fig. 26). However, expression levels were generally too low to be considered for further investigations.

The second lipase tested was PNPLA3. The membrane bound enzyme showed promising results as its mRNA expression levels in the area vasculosa were at average almost 3-fold higher than in the area vitellina and 4-fold higher than in the mesodermal blood vessel layer (Fig. 27).

Subsequently the investigation of LPL expression was performed. Expression levels showed very similar results in area vasculosa and vitellina tissue expression (Fig. 28), levels in the mesodermal cell layer turned out to be the lowest.

The next lipase to be tested was LAL. As shown in figure 29, it did not show the desired results as the lowest expression was measured in the area vasculosa and the highest in the mesodermal blood vessel layer.

The last lipase to be tested was HTGL. The obtained results were promising at a first sight as area vasculosa expression turned out to exceed the other measured tissues. Unfortunately the general expression levels were too low to draw any concrete conclusions (Fig. 30).

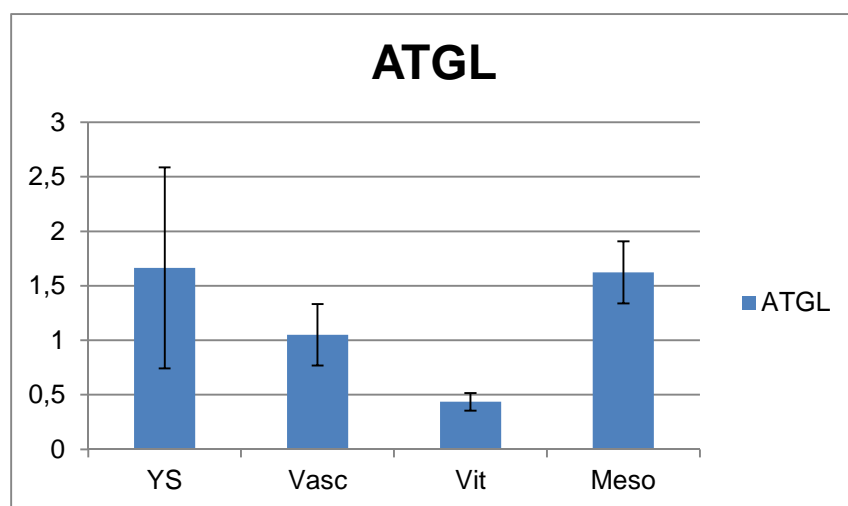


Figure 26. Levels of ATGL mRNA in total chicken YS, area vasculosa, area vitellina, and mesodermal blood vessel layer. QPCR experiments were performed after reverse transcription of total RNA from dissected 5d chicken YS tissue layers as described in the Materials and Methods section 2.6.2. Transcript levels are expressed as arbitrary units (AU) and represent the average of at least triplicate measurements \pm S.E.M.

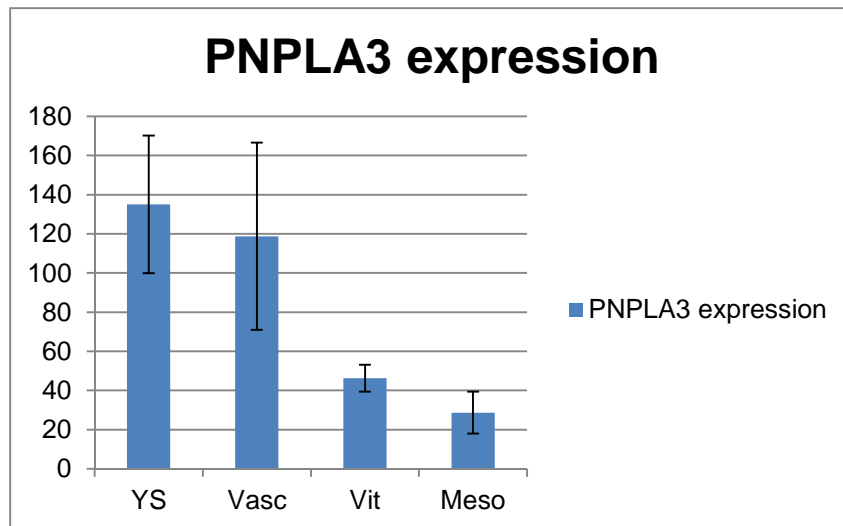


Figure 27. Levels of PNPLA3 mRNA in total chicken YS, area vasculosa, area vitellina, and mesodermal blood vessel layer. QPCR experiments were performed after reverse transcription of total RNA from dissected 5d chicken YS tissue layers as described in the Materials and Methods section 2.6.2. Transcript levels are expressed as arbitrary units (AU) and represent the average of at least triplicate measurements \pm S.E.M.

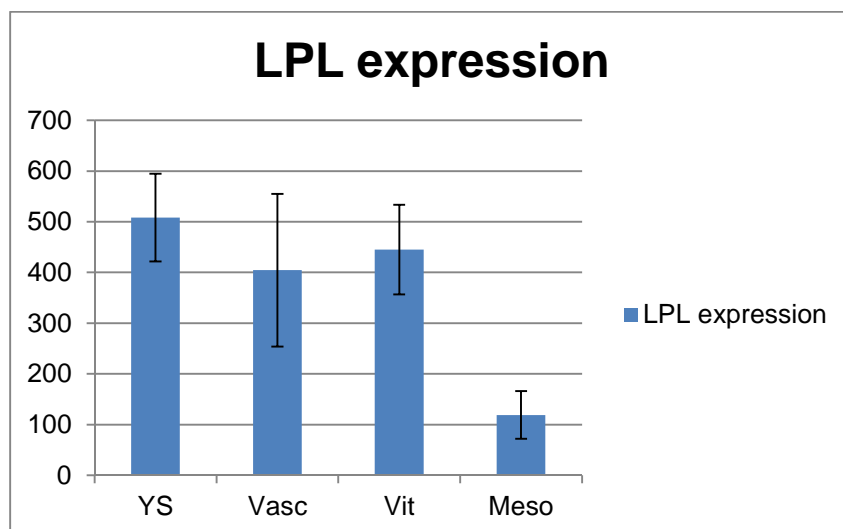


Figure 28. Levels of LPL mRNA in total chicken YS, area vasculosa, area vitellina, and mesodermal blood vessel layer. QPCR experiments were performed after reverse transcription of total RNA from dissected 5d chicken YS tissue layers as described in the Materials and Methods section 2.6.2. Transcript levels are expressed as arbitrary units (AU) and represent the average of at least triplicate measurements \pm S.E.M.

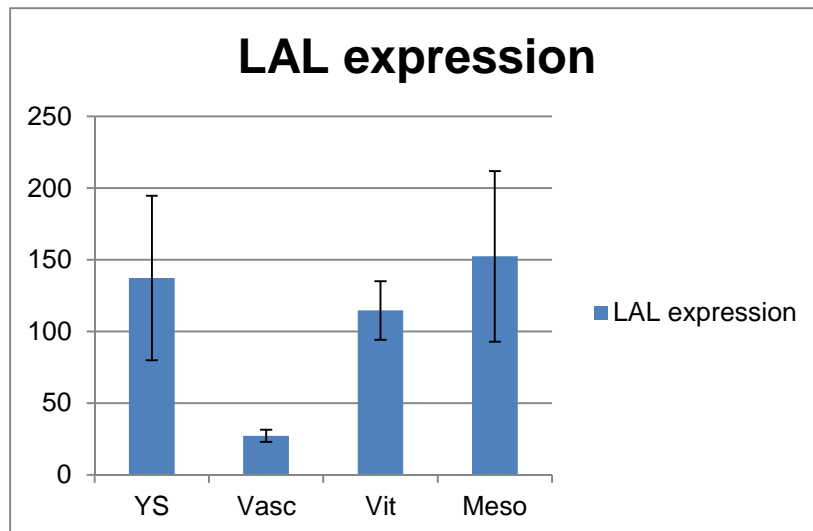


Figure 29. Levels of LAL mRNA in total chicken YS, area vasculosa, area vitellina, and mesodermal blood vessel layer. QPCR experiments were performed after reverse transcription of total RNA from dissected 5d chicken YS tissue layers as described in the Materials and Methods section 2.6.2. Transcript levels are expressed as arbitrary units (AU) and represent the average of at least triplicate measurements \pm S.E.M.

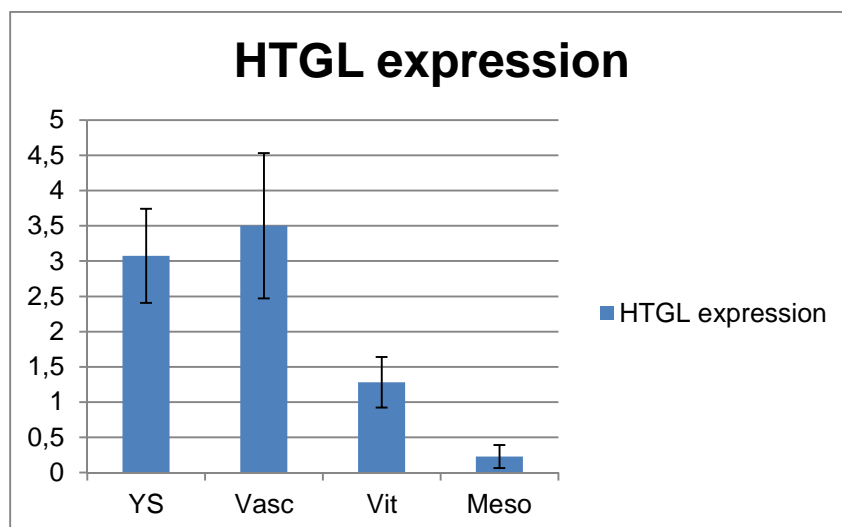


Figure 30. Levels of HTGL mRNA in total chicken YS area vasculosa, area vitellina, and mesodermal blood vessel layer. QPCR experiments were performed after reverse transcription of total RNA from dissected 5d chicken YS tissue layers as described in the Materials and Methods section 2.6.2. Transcript levels are expressed as arbitrary units (AU) and represent the average of at least triplicate measurements \pm S.E.M.

Finally, I compared expression levels of all investigated lipases to restrict the number of lipases possibly responsible for lipolysis of LDs in the area vasculosa. As indicated in figures 26 and 30, ATGL and HTGL were expressed only at very low level. LPL generally had the highest expression levels of all lipases but expression in the area vasculosa was lower than in the area vitellina (Fig. 28, and fig. 31). LAL showed the same trend between those two tissues like LPL (Fig. 29). PNPLA3 had in comparison to all observed tissues the highest mRNA levels in area vasculosa tissue samples (Fig 27). A specific antibody has to be created for future studies to confirm those findings also on protein level.

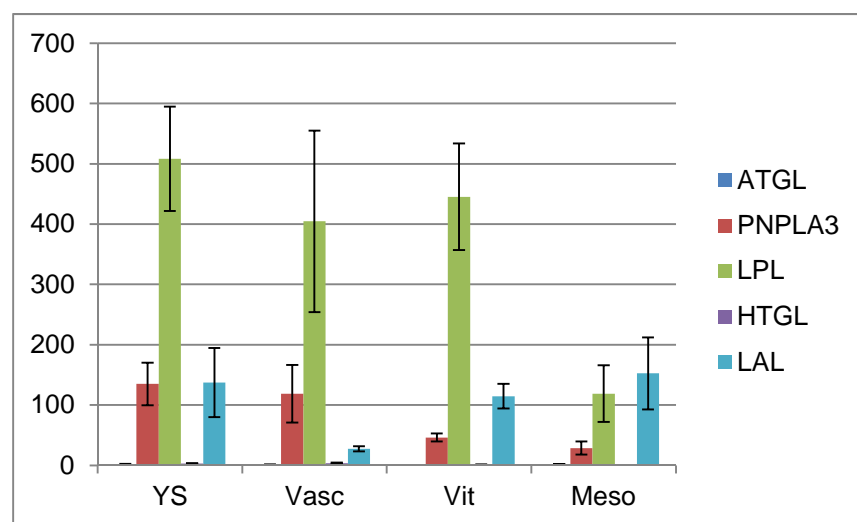


Figure 31. mRNA levels of all 5 investigated lipases indicated in distinct colors. Levels were measured in 5d chicken total YS, area vasculosa EECs, area vitellina EECs and mesodermal blood vessel layer. QPCR experiments were performed after reverse transcription of total RNA from dissected 5d chicken YS tissue layers as described in the Materials and Methods section (2.6.2). Transcript levels are expressed as arbitrary units (AU) and represent the average of at least triplicate measurements \pm S.E.M.

3.6 Investigation of lipase protein levels in the yolk sac

Due to a lack of time and consequent unavailability of specific antibodies I could only investigate the protein expression of one lipase. Our goat anti-chicken LPL antibody specifically detected a protein of approximately 55kDa, which is in good correlation with the predicted size of LPL protein found in literature, exclusively in the mesodermal blood vessel layer. These results contrast my experimental findings on RNA level, where I found LPL expression predominantly in area vasculosa and area vitellina tissue. However, the presence

of LPL protein in the mesodermal blood vessel layer supports the fact that LPL acts inside the capillary lumen therefore being not considerable as a TG-degrading lipase in the area vasculosa EECs (Fig. 32).

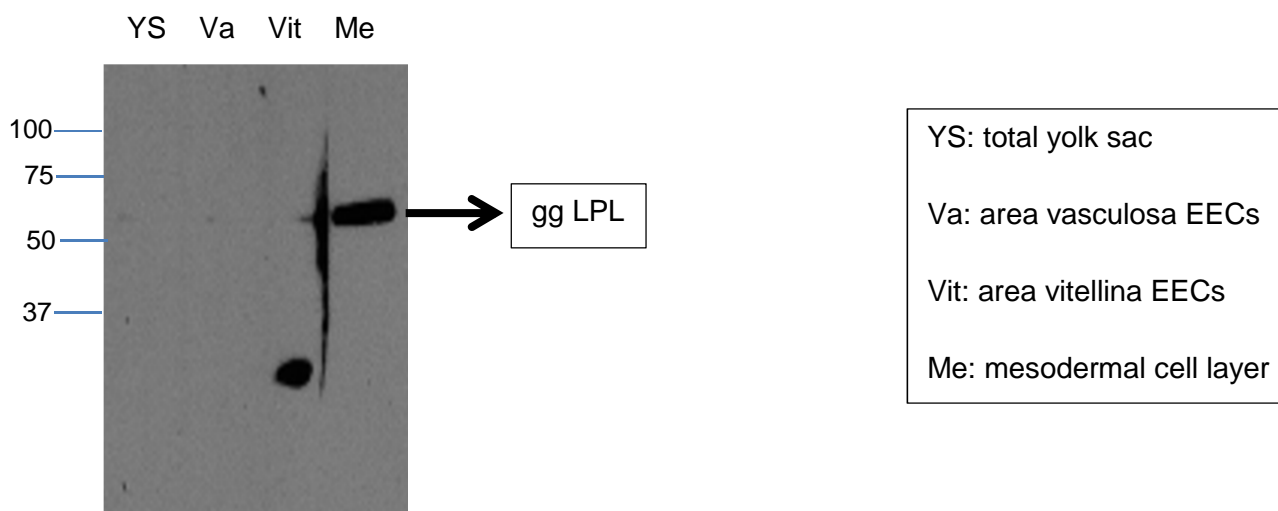


Figure 32. Western blot analysis under reducing conditions of total protein extracts shows the presence of LPL protein in the mesodermal cell layer. 50µg of total protein extracts from chicken YS, area vasculosa, area vitellina, and mesodermal blood vessel layer were subjected to a 12% SDS-PAA gel and blotted to nitrocellulose membrane. As primary antibody, a goat anti-chicken LPL antibody was used. As secondary antibody, HRP-conjugated rabbit anti-goat IgG was used. To visualize antibody binding ECL solution was applied.

In conclusion, only PNPLA3 mRNA levels showed a pattern suitable to be responsible for LD degradation in the area vasculosa (Fig. 27 and Fig. 31). As I could only investigate protein levels of LPL, the confirmation of found mRNA expression levels has to be postponed on future studies.

4. Discussion

The protein family of perilipins has gained increasing importance in lipid metabolism over the last decades. The number of family members steadily increased, and proteins with orthologous functions have been found in many different species and organisms. They were investigated in e.g. mammals, insects, slime molds, and fungi (Bickel, et al., 2009). Nevertheless there is not much known about PLINs in birds, let alone in the subspecies *G. g. domesticus*.

In this thesis I explored the involvement of PLINs in lipid storage and metabolism in the YS, an extraembryonic tissue involved in nutrient supply for the growing chick (Mobbs and McMillan, 1981; Speake et al., 1998).

Especially analyses of the EECs of the chicken YS 5d post-fertilization brought interesting new findings. PLIN1 did not show high expression levels in any part of the YS. Expression in the liver was also very low. As expected, PLIN1 expression in chicken adipose tissue was found to be high, as the values exceeded those in liver and YS by more than a hundredfold (Fig. 11). These results are in perfect agreement with findings of many previous studies on PLIN1, which showed that the expression is restricted to adipose tissue and steroidogenic cells (Servetnick et al., 1991; Blanchette-Mackie et al., 1995).

Completely different and surprising results showed PLIN2 investigations at the mRNA level. PLIN2 was the only gene of the investigated PLINs which showed detectable expression in the YS. Despite the fact that compared to liver and adipose tissue, PLIN2 expression was lowest in the YS (Fig. 12), PLIN2 mRNA levels were hundredfold increased compared to PLIN1 and PLIN3 (Fig. 13). Dissection of the YS into its distinct cell layers revealed that, in contrast to many other yet identified genes (Nakazawa et al., 2011) PLIN2 mRNA levels were highest in the area vitellina of the developing YS. Furthermore, I investigated PLIN2 protein levels in the YS. To do so, I used an anti-human PLIN2 polyclonal antibody directed against a human PLIN2 epitope with over 75% identity to the chicken PLIN2 sequence. In agreement with the findings at the mRNA level, I found PLIN2 protein only present in the area vitellina of the YS.

The area vitellina of the early developing chicken YS consists of an ectodermal cell layer and the underlying EECs, which are in direct contact with the yolk compartment. The main difference compared to the area vasculosa is that the area vitellina lacks the mesodermal blood vessel layer that overgrows the EECs with proceeding development. The leading edge of the area vasculosa is defined by the sinus terminalis, which clearly separates the area

vasculosa from the area vitellina (Fig. 1). The area vasculosa was described by many previously published reports (Refs) as the functional unit of the YS, being able to take up and ultimately provide the growing embryo with nutrients from the yolk. This transport of nutrients can only be accomplished with a well-established circulation from the YS to the embryo, which is absent in the area vitellina. Additionally, the secretion of TG-rich apoB containing lipoproteins was detected in EECs of the area vasculosa, but was completely absent in the area vitellina (R. Bauer, unpublished data). Nascent lipoproteins are assembled by utilizing TGs and phospholipids from LDs, which eventually are secreted and serve as energy supply for the growing embryo. However, besides the fact that area vitellina EECs exhibit extensive lipid storing in LDs which occupy major parts of the cytosol (Fig. 2), VLDL secretion seems to be somehow blocked.

PLIN2 is a LD associated protein and it seems to be the only PLIN expressed in the area vitellina EECs (the non-investigated PLIN4 and PLIN5 excluded). Importantly, immunofluorescence experiments with cultivated EECs derived from the area vitellina indeed confirmed an association of PLIN2 with the LD surface (Fig. 23). The connection between lipid storage in the area vitellina and VLDL-mediated secretion of stored lipids in the area vasculosa could partially be explained by findings in previous mouse and rat studies (Chang, et al., 2010; Magnusson, et al., 2006). In a mouse obesity model, assembly and secretion of VLDL was upregulated when PLIN2 expression was knocked out, resulting in an improvement of the fatty liver. Additionally the expression of MTTP, the crucial VLDL assembly factor, was highly increased. The authors suggested that in absence of PLIN2, MTTP-triggered VLDL assembly and increased TG secretion was facilitated (Chang, et al., 2010). On the other hand, PLIN2 overexpression caused a decrease in VLDL secretion of incorporated TGs (magnussen et al., 2006).

In the developing chicken YS, the presence or absence of PLIN2 also seems to have a profound impact on VLDL secretion rates. PLIN2 covers the LD surface in EECs of the area vitellina, where no VLDL secretion can be observed. However, during the transition from the area vitellina to the area vasculosa, PLIN2 expression disappears, and LDs are no longer covered by PLIN2. Therefore, I assume that in the PLIN2-deficient EECs of the area vasculosa, LDs serve as TG store for VLDL synthesis and secretion. Possibly, removal of PLIN2 from the LDs somehow alters the accessibility of the LD surface in a way that the stored TGs within can be utilized for VLDL assembly. Further studies are required to elucidate the molecular mechanisms regulating this important metabolic switch in terms of embryo nourishment. Additionally it might be of interest and great importance to test MTTP gene expression and protein levels in EECs of the area vasculosa and the area vitellina to get a better understanding of the regulation of VLDL secretion in the chicken YS.

PLIN3 was found to be expressed in almost all tissues. It showed very similar but low expression levels in adipose tissue, liver, and YS. The expression values led to the conclusion that PLIN3 likely does not play a significant role in controlling lipid metabolism in the early chicken YS.

Due to lack of chicken PLIN4 and PLIN5 coding sequences, I could not perform any investigations on these genes and their products. In other species, PLIN4 and PLIN5 are, like PLIN1, predominantly expressed in adipose tissue. PLIN4 is predominantly involved in long-time storage of lipids in white adipose tissue (Wolins et al., 2003). As it was also found associated with small evolving LDs, it might also work in concert together with PLIN2 by means of building up LDs and maintaining constant lipid storage. PLIN5 was shown to be expressed predominantly in adipocytes of brown adipose tissue, which has a high rate of β -oxidation and is required for quick energy access. (Dalen, et al., 2006). Hopefully, avian PLIN4 and PLIN5 genes, if indeed existing, will be discovered and/or sequenced soon, so their possible role(s) in lipid storage in the YS can be solved.

The transition from area vitellina to area vasculosa is accompanied by increased metabolism via lipoprotein secretion, mainly in the form of apoB-containing TG-rich lipoproteins (Bauer et al., 2012, unpublished data). Additionally, the presence of large cytosolic LDs in the EECs raised the question whether YS-specific lipid hydrolases/lipases are involved in the mobilization process of TG-stores in the area vasculosa for subsequent re-esterification and utilization in VLDL assembly. Therefore, I tested for the presence of a number of TG lipases that could mediate the rate-determining step of lipolysis. According to findings in literature all investigated lipases perform TG hydrolyzing actions. LAL, a lipid hydrolyzing enzyme located in the cell's lysosomes is able to perform this rate determining step. My investigations at the mRNA level with qPCR showed the lowest expression values in the area vasculosa tissue. LAL levels in the area vitellina were more than 4 times higher and levels in the mesodermal blood vessel layer were 6 times higher. Therefore, LAL is unlikely to be involved in the mobilization of TG stores for VLDL assembly in the area vasculosa of the chicken YS.

A lipase that has great impact on metabolism of VLDL and chylomicrons in adipose tissue is LPL. Even though LPL is attached to endothelial membranes I found LPL to be expressed to the highest extent in the EECs of the area vasculosa and area vitellina. In contrast, protein levels detected by Western blot confirmed published data, since LPL was only found in samples of the mesodermal blood vessel layer, thus also excluding LPL as a candidate lipase.

A lipase related to LPL is HTGL (Hide, et al., 1992). It has a great impact on lipoprotein turnover. However, the expression levels were generally very low. Therefore, this lipase also is rather unlikely to represent a proper candidate enzyme for this metabolic challenge.

ATGL was found to be one of the rate-determining enzymes in TG breakdown in adipose tissue (reviewed in Smirnova, et al., 2006). This fact seemed to fit to the results of my investigation. Expression levels indicated that ATGL may not be the predominant lipase in the EECs of the area vasculosa. The values in the mesodermal blood vessel layer turned out to exceed the expression in the EECs. Additionally, the general expression levels were like the ones for HTGL too low to be distinguished from background signal (Fig. 26). Therefore its functions also were not considered as crucial for TG hydrolysis in the chicken YS.

PNPLA3, a TG-lipase is, like its protein family member ATGL, highly expressed during adipocyte differentiation (Baulande, et al., 2001). Nevertheless, it was shown that PNPLA3 is regulated by complete opposite feeding statuses. Fasting decreased mRNA levels in rats, whereas ATGL on the other hand was upregulated (Oliver, et al., 2012). The same outcome was observed in laying hens as mRNA expression of PNPLA3 in the liver was diminished by fasting and highly increased after refeeding (Riegler, et al., 2011).

PNPLA3 expression levels in this study showed highest values in area vasculosa (Fig. 27). Only PNPLA3 would be a favorable candidate for further studies on the protein. I assume that PNPLA3 possibly could play a crucial role in the TG turnover in LDs of the area vasculosa. As PLIN2 seems to be involved in LD protecting functions in the area vitellina, its total absence in the area vasculosa could have effects promoting TG-hydrolysis mediated by PNPLA3. Secretion of TG-rich, apoB-containing VLDL particles (Bauer, et al., 2012, unpublished data) was recently detected in the EECs of the area vasculosa of the chicken YS, but not in the area vitellina. PNPLA3 again is supposed to hydrolyze TGs from LDs which then are re-esterified in the ER and Golgi. These newly synthesized TGs can then be transferred to apoB during the VLDL maturation process in the secretory pathway (Pirazzi, et al., 2012). Clearly, more detailed research on PNPLA3 at the protein level has to be done to reveal its involvement in lipid metabolism. All of the other investigated lipases seem to play either a minor role concerning lipolysis, mainly based on their low expression levels, or they are expressed in the metabolically less active area vitellina. Further candidates, probably involved in TG hydrolysis in the EECs of the chicken YS, may emerge in future studies.

5. References

- Akter M. H., Y. T. (2008). Perilipin, a critical regulator of fat storage and breakdown, is a target gene of estrogen receptor-related receptor alpha. *Biochem Biophys Res Commun.*368(3):563-568.
- Anderson R. A., B. G. (1999). Lysosomal acid lipase mutations that determine phenotype in Wolman and cholesterol ester storage disease. *Mol Genet Metab.*68(3):333-345.
- Arimura N., H. T. (2004). The peroxisome proliferator-activated receptor gamma regulates expression of the perilipin gene in adipocytes. *J Biol Chem.*279(11):10070-10076.
- Aslanidis C., R. S. (1996). Genetic and biochemical evidence that CESD and Wolman disease are distinguished by residual lysosomal acid lipase activity. *Genomics.*33(1):85-93.
- Bahr, J. M. (2008). *The Chicken as a Model Organism from Sourcebook of Models for Biomedical Research* edited by Conn, M., P. Totowa NJ: Humana Press.
- Barbero P., B. E. (2001). TIP47 is not a component of lipid droplets. *J Biol Chem.*276(26):24348-24351.
- Bartz R., Z. J. (2007). Dynamic activity of lipid droplets: protein phosphorylation and GTP-mediated protein translocation. *J Proteome Res.*6(8):3256-3265.
- Baulande S., L. F. (2001). Adiponutrin, a transmembrane protein corresponding to a novel dietary- and obesity-linked mRNA specifically expressed in the adipose lineage. *J Biol Chem.*276(36):33336-33344.
- Bensadoun B. (1999). Lipoprotein lipase. *Annu Rev Nutr.*:217-237.
- Bickel P. E., T. J. (2009). PAT proteins, an ancient family of lipid droplet proteins that regulate cellular lipid stores. *Biochim Biophys Acta.*1791(6):419-440.
- Blanchette-Mackie E. J., D. N. (1995). Perilipin is located on the surface layer of intracellular lipid droplets in adipocytes. *J Lipid Res.*36(6):1211-1226.
- Boström P., A. L.-R. (2007). SNARE proteins mediate fusion between cytosolic lipid droplets and are implicated in insulin sensitivity. *Nat Cell Biol.*9(11):1286-1293.

- Boström P., R. M. (2005). Cytosolic lipid droplets increase in size by microtubule-dependent complex formation. *Arterioscler Thromb Vasc Biol.*25(9):1945-1951.
- Brasaemle D. L., B. T. (1997). Post-translational regulation of perilipin expression. Stabilization by stored intracellular neutral lipids. *J Biol Chem.*272(14):9378-9387.
- Brasaemle D. L., B. T.-M. (1997). Adipose differentiation-related protein is an ubiquitously expressed lipid storage droplet-associated protein. *J Lipid Res.*38(11):2249-2263.
- Brasaemle D. L., D. G. (2004). Proteomic analysis of proteins associated with lipid droplets of basal and lipolytically stimulated 3T3-L1 adipocytes. *J Biol Chem.*279(45):46835-46842.
- Brown J. M., C. S. (2007). CGI-58 facilitates the mobilization of cytoplasmic triglyceride for lipoprotein secretion in hepatoma cells. *J Lipid Res.*48(10):2295-2305.
- Brown W. R., H. J. (2003). The chicken as a model for large-scale analysis of vertebrate. *Nat Rev Genet.*4(2):87-98.
- Bussell R. Jr., E. D. (2003). A structural and functional role for 11-mer repeats in alpha-synuclein and other exchangeable lipid binding proteins. *J Mol Biol.*329(4):763-778.
- Chang B. H., L. L. (2010). Absence of adipose differentiation related protein upregulates hepatic VLDL secretion, relieves hepatosteatosis, and improves whole body insulin resistance in leptin-deficient mice. *J Lipid Res.*51(8):2132-2142.
- Dalen K. T., D. T. (2007). LSDP5 is a PAT protein specifically expressed in fatty acid oxidizing tissues. *Biochim Biophys Acta.*1771(2):210-227.
- Dalen K. T., S. ..-F. (2004). Adipose tissue expression of the lipid droplet-associating proteins S3-12 and perilipin is controlled by peroxisome proliferator-activated receptor-gamma. *Diabetes.*53(5):1243-1252.
- Datta S, L. C. (1988). Human hepatic lipase. Cloned cDNA sequence, restriction fragment length polymorphisms, chromosomal localization, and evolutionary relationships with lipoprotein lipase and pancreatic lipase. *J Biol Chem.*263(3):1107-1110.
- Díaz E., P. S. (1998). TIP47: a cargo selection device for mannose 6-phosphate receptor trafficking. *Cell.*93(3):433-443.
- Du H., C. T. (2008). Wolman disease/cholesteryl ester storage disease: efficacy of plant-produced human lysosomal acid lipase in mice. *J Lipid Res.*9(8):1646-1657.

- Du H., H. M. (2001). Lysosomal acid lipase-deficient mice: depletion of white and brown fat, severe hepatosplenomegaly, and shortened life span. *J Lipid Res.*42(4):489-500.
- Du H., W. D. (1996). Tissue and cellular specific expression of murine lysosomal acid lipase mRNA and protein. *J Lipid Res.*37(5):937-949.
- Dugi K. A., D. H.-F. (1995). Human hepatic and lipoprotein lipase: the loop covering the catalytic site mediates lipase substrate specificity. *J Biol Chem.*270(43):25396-25401.
- Edvardsson U., L. A.-O.-S. (2006). PPARalpha activation increases triglyceride mass and adipose differentiation-related protein in hepatocytes. *J Lipid Res.*47(2):329-340.
- Ehehalt R., F. J. (2006). Translocation of long chain fatty acids across the plasma membrane--lipid rafts and fatty acid transport proteins. *Mol Cell Biochem.*284(1-2):135-140.
- Fujimoto Y., I. H. (2004). Identification of major proteins in the lipid droplet-enriched fraction isolated from the human hepatocyte cell line HuH7. *Biochim Biophys Acta.*1644(1):47-59.
- Fujimoto Y., I. H. (2007). Involvement of ACSL in local synthesis of neutral lipids in cytoplasmic lipid droplets in human hepatocyte HuH7. *J Lipid Res.*48(6):1280-1292.
- Gao J., Y. H. (2000). Stimulation of adipose differentiation related protein (ADRP) expression in adipocyte precursors by long-chain fatty acids. *J Cell Physiol.*182(2):297-302.
- Garcia A., S. A. (2003). The central domain is required to target and anchor perilipin A to lipid droplets. *J Biol Chem.*278(1):625-35.
- Goldstein J. L., D. S. (1975). Role of lysosomal acid lipase in the metabolism of plasma low density lipoprotein. Observations in cultured fibroblasts from a patient with cholesteryl ester storage disease. *J Biol Chem.*250(21):8487-8495.
- Greenberg A. S., E. J. (1993). Isolation of cDNAs for perilipins A and B: sequence and expression of lipid droplet-associated proteins of adipocytes. *Proc Natl Acad Sci U S A.*90(24):12035-12039.
- Greenberg A. S., E. J.-M. (1991). Perilipin, a major hormonally regulated adipocyte-specific phosphoprotein associated with the periphery of lipid storage droplets. *J Biol Chem.*266(17):11341-11346.
- Guo Y., C. K. (2009). Lipid droplets at a glance. *J Cell Sci.*122(Pt 6):749-752.

- Guo Y., W. T. (2008). Functional genomic screen reveals genes involved in lipid-droplet formation and utilization. *Nature*.453(7195):657-661.
- Hammersen F., H. F. (1985). *Histology, color atlas of microscopic anatomy*. Urban & Schwarzenberg, Baltimore 2nd ed.
- Hickenbottom S. J., K. A. (2004). Structure of a lipid droplet protein; the PAT family member TIP47. *Structure*.12(7):1199-1207.
- Hide W. A., C. L. (1992). Structure and evolution of the lipase superfamily. *J Lipid Res*.33(2):167-178.
- Huang Y., H. S. (2010). A feed-forward loop amplifies nutritional regulation of PNPLA3. *Proc Natl Acad Sci U S A*.107(17):7892-7897.
- Jenkins C. M., M. D. (2004). Identification, cloning, expression, and purification of three novel human calcium-independent phospholipase A2 family members possessing triacylglycerol lipase and acylglycerol transacylase activities. *J Biol Chem*.279(47):48968-48975.
- Jiang H. P., S. G. (1992). Isolation and characterization of a full-length cDNA coding for an adipose differentiation-related protein. *Proc Natl Acad Sci U S A*.89(17):7856-7860.
- Kershaw E. E., H. J. (2006). Adipose triglyceride lipase: function, regulation by insulin, and comparison with adiponutrin. *Diabetes*.55(1):148-157.
- Kinnunen P. K., J. R. (1977). Activation of lipoprotein lipase by native and synthetic fragments of human plasma apolipoprotein C-II. *Proc Natl Acad Sci U S A*.74(11):4848-4851.
- Komiyama T., K. I. (2004). Japanese domesticated chickens have been derived from Shamo traditional fighting cocks. *Mol Phylogenet Evol*.33(1):16-21.
- Ladjali-Mohammed K, B. J.-B. (1999). International system for standardized avian karyotypes (ISSAK): standardized banded karyotypes of the domestic fowl (*Gallus domesticus*). *Cytogenet Cell Genet*.86(3-4):271-276.
- Lass A., Z. R. (2006). Adipose triglyceride lipase-mediated lipolysis of cellular fat stores is activated by CGI-58 and defective in Chanarin-Dorfman Syndrome. *Cell Metab*.3(5):309-319.
- Liu P., B. R. (2007). Rab-regulated interaction of early endosomes with lipid droplets. *Biochim Biophys Acta*.1773(6):784-793.

- Liu P., B. R. (2008). Rab-regulated membrane traffic between adiposomes and multiple endomembrane systems. *Methods Enzymol.*439:327-337.
- Londos C., B. D. (1999). Perilipins, ADRP, and other proteins that associate with intracellular neutral lipid droplets in animal cells. *Semin Cell Dev Biol.*10(1):51-58.
- Magnusson B., A. L.-B. (2006). Adipocyte differentiation-related protein promotes fatty acid storage in cytosolic triglycerides and inhibits secretion of very low-density lipoproteins. *Arterioscler Thromb Vasc Biol.*26(7):1566-1571.
- Martin S., P. R. (2006). Lipid droplets: a unified view of a dynamic organelle. *Nat Rev Mol Cell Biol.*7(5):373-378.
- Martinez-Botas J, A. J. (2000). Absence of perilipin results in leanness and reverses obesity in *Lepr(db/db)* mice. *Nat Genet.*26(4):474-479.
- Mobbs I. G., M. D. (1981). Transport across endodermal cells of the chick yolk sac during early stages of development. *Am J Anat.*;160(3):285-308.
- Nakamura N., F. T. (2003). Adipose differentiation-related protein has two independent domains for targeting to lipid droplets. *Biochem Biophys Res Commun.*;306(2):333-338.
- Nakazawa F., C. A. (2011). Yolk Sac Endoderm Is the Major Source of Serum Proteins and Lipids and Is Involved in the Regulation of Vascular Integrity in Early Chick Development. *Dev Dyn.*240(8):2002-2010.
- Ohsaki Y., M. T.-S. (2006). Recruitment of TIP47 to lipid droplets is controlled by the putative hydrophobic cleft. *Biochem Biophys Res Commun.*347(1):279-287.
- Oliver P., C. A.-R. (2012). Diet-induced obesity affects expression of adiponutrin/PNPLA3 and adipose triglyceride lipase, two members of the same family. *Int J Obes (Lond).*36(2):225-232.
- O'Sullivan N. P., D. E. (1991). Relationships among age of dam, egg components, embryo lipid transfer, and hatchability of broiler breeder eggs. *Poult. Sci.*70.:2180–2185.
- Pasteur, L. (1880). The attenuation of the causal agent of fowl cholera. *Les Comptes Rendus de l'Académie des sciences; Vol. 91:*637-680.
- Paul A., C. B. (2008). Deficiency of adipose differentiation-related protein impairs foam cell formation and protects against atherosclerosis. *Circ Res.*102(12):1492-1501.

- Pilch P. F., S. R. (2007). Cellular spelunking: exploring adipocyte caveolae. *J Lipid Res.*(10):2103-2111.
- Pirazzi C., A. M.-M. (2012). Patatin-like phospholipase domain-containing 3 (PNPLA3) I148M (rs738409) affects hepatic VLDL secretion in humans and in vitro. *J Hepatol. pii: S0168-8278(12)00606-X. doi: 10.1016/j.jhep.2012.07.030.*
- Ploegh, H. (2007). A lipid-based model for the creation of an escape hatch from the endoplasmic reticulum. *Nature.*448(7152):435-438.
- Riegler B., B. C. (2011). Enzymes involved in hepatic acylglycerol metabolism in the chicken. *Biochem Biophys Res Commun.*406(2):257-261.
- Rydel T. J., W. J. (2003). The crystal structure, mutagenesis, and activity studies reveal that patatin is a lipid acyl hydrolase with a Ser-Asp catalytic dyad. *Biochemistry.*42(22):6696-6708.
- Saito H., D. P.-K. (2001). Lipid binding-induced conformational change in human apolipoprotein E. Evidence for two lipid-bound states on spherical particles. *J Biol Chem.*;276(44):40949-40954.
- Santamarina-Fojo S., H. C. (2000). Role of hepatic and lipoprotein lipase in lipoprotein metabolism and atherosclerosis: studies in transgenic and knockout animal models and somatic gene transfer. *Int J Tissue React.*22(2-3):39-47.
- Sato K., A. Y. (1999). Lipoprotein hydrolysis and fat accumulation in chicken adipose tissues are reduced by chronic administration of lipoprotein lipase monoclonal antibodies. *Poult Sci.*78(9):1286-1291.
- Schaffer, J. (2003). Lipotoxicity: when tissues overeat. *Curr Opin Lipidol.*14(3):281-287.
- Scherer P. E., B. P. (1998). Cloning of cell-specific secreted and surface proteins by subtractive antibody screening. *Nat Biotechnol.*16(6):581-586.
- Schmuth M., H. C.-Q. (2004). Peroxisome proliferator-activated receptor (PPAR)-beta/delta stimulates differentiation and lipid accumulation in keratinocytes. *J Invest Dermatol.*122(4):971-983.
- Servetnick D. A., B. D.-G. (1995). Perilipins are associated with cholesteryl ester droplets in steroidogenic adrenal cortical and Leydig cells. *J Biol Chem.*270(28):16970-16973.
- Sheng G. (2010). Primitive and definitive erythropoiesis in the yolk sac: a bird's eye view. *Int. J. Dev. Biol.* 54:1033-1043.

- Smirnova E., G. E. (2006). ATGL has a key role in lipid droplet/adiposome degradation in mammalian cells. *EMBO Rep.* 7(1):106-113.
- Speake B. K., M. A. (1998). Transport and transformations of yolk lipids during development of the avian embryo. *Prog Lipid Res* 37:1-32.
- Stern C. D. (2005). The chick: A great model system becomes even greater. *Dev Cell.* 8(1):9-17.
- Sturmey R. G., O. P. (2006). Fluorescence resonance energy transfer analysis of mitochondrial:lipid association in the porcine oocyte. *Reproduction.* 132(6):829-837.
- Subramanian V., G. A. (2004). Hydrophobic sequences target and anchor perilipin A to lipid droplets. *J Lipid Res.* 45(11):1983-1991.
- Sztalryd C., B. M. (2006). Functional compensation for adipose differentiation-related protein (ADFP) by Tip47 in an ADFP null embryonic cell line. *J Biol Chem.* 281(45):34341-34348.
- Tauchi-Sato K., O. S. (2002). The surface of lipid droplets is a phospholipid monolayer with a unique Fatty Acid composition. *J Biol Chem.* 277(46):44507-44512.
- Turró S., I.-T. M. (2006). Identification and characterization of associated with lipid droplet protein 1: A novel membrane-associated protein that resides on hepatic lipid droplets. *Traffic.* 7(9):1254-1269.
- Vieira S. L., a. E. (1998). Broiler Yields Using Chicks from Egg Weight Extremes and Diverse Strains. *J. Appl. Poult. Res.* 7:372–376.
- Villena J. A., R. S.-N. (2004). Desnutrin, an adipocyte gene encoding a novel patatin domain-containing protein, is induced by fasting and glucocorticoids: ectopic expression of desnutrin increases triglyceride hydrolysis. *J Biol Chem.* 279(45):47066-47075.
- Walther T. C., F. R. (2008). The life of lipid droplets. *Biochim Biophys Acta.* 1791(6):459-466.
- Wang H., B. M. (2011). Unique regulation of adipose triglyceride lipase (ATGL) by perilipin 5, a lipid droplet-associated protein. *J Biol Chem.* 286(18):15707-15715.
- Wolins N. E., Q. B. (2005). S3-12, Adipophilin, and TIP47 package lipid in adipocytes. *J Biol Chem.* 280(19):19146-19155.
- Wolins N. E., Q. B.-B. (2006). OXPAT/PAT-1 is a PPAR-induced lipid droplet protein that promotes fatty acid utilization. *Diabetes.* 55(12):3418-3428.

- Wolins N. E., R. B. (2001). TIP47 associates with lipid droplets. *J Biol Chem.*276(7):5101-5108.
- Wolins N. E., S. J. (2003). Adipocyte protein S3-12 coats nascent lipid droplets. *J Biol Chem.*278(39), S. 37713-37721.
- Xu G., S. C. (2005). Post-translational regulation of adipose differentiation-related protein by the ubiquitin/proteasome pathway. *J Biol Chem.*280(52):42841-42847.
- Xu G., S. C. (2006). Degradation of perilipin is mediated through ubiquitination-proteasome pathway. *Biochim Biophys Acta.*;1761(1):83-90.
- Yamaguchi T., O. N. (2004). CGI-58 interacts with perilipin and is localized to lipid droplets. Possible involvement of CGI-58 mislocalization in Chanarin-Dorfman syndrome. *J Biol Chem.*279(29):30490-30497.
- Zhang L., L. A. (2005). Calcium triggers folding of lipoprotein lipase into active dimers. *J Biol Chem.*280(52):42580-42591.
- Zimmermann R., S. J.-G. (2004). Fat mobilization in adipose tissue is promoted by adipose triglyceride lipase. *Science.*306(5700):1383-1386.

6. List of abbreviations

A

α	alpha, anti
APS	ammonium persulfate
AMP	ampicillin
ATGL	adipose triglyceride lipase
ATP	adenosine tri-phosphate
apoE	apolipoprotein E
apoB	apolipoprotein B
au	arbitrary units

B

bp	basepairs
BODIPY	boron-dipyrromethene
BAT	brown adipose tissue
BSA	bovine serum albumine

C

CE	cholesteryl ester
CM	chylomicrons
CaCl ₂	calcium chloride
C-terminus	carboxy-terminus
CCT	cytidyltransferase
cAMP	cyclic adenosine mono-phosphate
CGI-58	Comparative Gene Identification-58

CDS	Chanarin Dorfman Syndrome
CESD	cholesterol ester storage disease
ChCl ₃	chloroform
CoA	Coenzyme A
D	
DNA	deoxyribonucleic acid
DTT	dithiotreitol
DAPI	4',6-diamidino-2-phenylindole
DGAT	diacylglycerol acyltransferase
dNTP	deoxyribonucleotide triphosphates
ddH ₂ O	double deionized water
E	
ECL	enhanced chemiluminescence
ER	endoplasmatic reticulum
EEC	endodermal epithelial cell
ERRα	estrogen receptor-related receptor alpha
E.coli	<i>Escherichia coli</i>
EDTA	ethylenediaminetetraacetic acid
EGFP	enhanced green fluorescent protein
EtOH	ethanol
F	
FFA	free fatty acid
G	
gg	gallus gallus

g	gram
GAPDH	glyceraldehyde 3-phosphate dehydrogenase
xg	gravity
H	
HDL	high density lipoprotein
HRP	horseradish peroxidase
h	hour
HTGL	hepatic triglyceride lipase
HCL	hydrogen chloride
I	
IgG	immunoglobuline G
K	
kDa	kilo Dalton
kg	kilo gram
KCl	potassium chloride
Kan	Kanamycin
L	
LDL	low density lipoprotein
LDLR	low density lipoprotein receptor
LPL	lipoprotein lipase
LAL	lysosomal acid lipase
LH	laying hen
LD	lipid droplet

M

μ	micro
mM	millimolar
mA	milliampere
mRNA	messenger ribonucleic acid
MTTP	microsomal triglyceride transfer protein
M6P	mannose 6-phosphate receptor
MeOH	methanol
MgCl ₂	magnesium chloride

N

nm	nanometer
N-terminus	amino terminus
NAFL	non-alcoholic fatty liver disease
NaCl	sodium chloride

O

O/N	overnight
OD	optical density

P

RT-PCR	reverse transcriptase polymerase chain reaction
qPCR	quantitative real time PCR
PBS	phosphate-buffered saline
PAA	polyacrylamide
PAGE	polyacrylamide gel electrophoresis
PPAR	peroxisome proliferator-activated receptor

PNPLA3	patatin-like phospholipase domain-containing protein
PKA	protein kinase A
PAT	Perilipin, ADRP, TIP47
R	
R/T	room temperature
rpm	revolutions per minute
RNA	ribonucleic acid
S	
SDS	sodium dodecyl sulphate
SNARE	soluble NSF attachment protein receptor
siRNA	small interfering ribonucleic acid
S.E.M.	standard error of the mean
T	
TG	triglyceride
TEMED	Tetramethylethylenediamine
TBS	tris buffered saline
TAE	tris, acetic acid and EDTA
U	
UV	ultraviolet
V	
VLDL	very-low density lipoprotein
W	

WD	Wolman's disease
WAT	white adipose tissue
w/v	weight per volume
X	
X-Gal	5-bromo-4-chloro-indolyl- β -D-galactopyranoside
Y	
YS	yolk sac

Abstract

The chicken is a very important model organism. It belongs, like all other birds, reptiles, and amphibians to the group of oviparous animals that lay eggs, resulting in an almost completely separated embryonic development outside the mother's body. Therefore, especially the chicken embryo is very suitable for developmental and nutritional studies. The chicken yolk sac (YS) of the developing embryo plays a crucial role in nutrient transfer processes. It functions as a kind of digestive system to provide the embryo with nutrients taken up from the YS-enclosed yolk. It is built up by 2 different cell types. The bottom layer, which is in direct contact to the yolk, consists of an epithelium of endodermal cells which take up essential components provided by the yolk. On top of these endodermal epithelial cells (EECs) lies a mesodermal layer, comprising a blood vessel layer endothelium that transports mobilized nutrients to the developing embryo. With ongoing development, the mesodermal blood vessel layer overgrows and covers the entire EEC layer, in this state named area vasculosa. However, in the first few days after egg deposition the YS contains a significant part of uncovered EECs, which is called area vitellina.

In this study I found that the EECs of the area vitellina are of great importance for intracellular lipid storage in cellular organelles called lipid droplets (LDs). The large amounts of lipids, retained for later mobilization to the embryo, are packaged in phospholipid monolayer-enclosed spherical LDs. They consist of neutral lipids, such as triglycerides (TGs) and cholesteryl esters (CEs).

The mRNA level, measured by qPCR, of PLIN2 (also called ADRP), a member of a family of LD-associated proteins (the PLINs), was found to be particularly high in the chicken YS. Interestingly, I observed high levels in the unvascularized EECs of the area vitellina, but not in the developmentally advanced vascularized area (the area vasculosa). In many mammalian species PLIN2, not yet demonstrated in the chicken, was found to be associated with nascent LDs and involved in lipid storage. Expression of other PLINs could not be detected in this study.

Using Western blotting technique, the protein levels of PLIN2 were determined. The results also point to an important role in the storage of the huge amounts of LDs in the EECs of the area vitellina. The direct association of PLIN2 to the LDs of the EECs of the area vitellina could be visualized by anti-PLIN2 immuno-staining of the area vitellina EECs and subsequent confocal microscopy.

After detecting PLIN2, a very potent protein concerning the intracellular storage of neutral lipids, I attempted to reveal how these lipids could be utilized for embryonic nutrition. I searched for (a) lipid hydrolyzing enzyme(s) with specificity for TG hydrolysis, as this is the starting point for degradation of stored lipids. I investigated various TG hydrolyzing enzymes at the mRNA level with qPCR, and could indeed detect one. The candidate is a membrane bound enzyme called Patatin-like phospholipase domain-containing protein (PNPLA3). Indeed, evidence for a role in TG hydrolysis in the YS for PNPLA3 is provided by showing increased expression rates in the area vasculosa, i.e., the metabolically more active tissue. The area vasculosa is very likely also the region from which the nutrients are delivered via the mesodermal blood vessels to the embryo.

Zusammenfassung

Das Haushuhn ist ein sehr wichtiger Modellorganismus. Es gehört, wie alle Vogelarten, Amphibien und Reptilien zu der Gruppe von oviparen Tieren, die Eier legen und bei denen somit beinahe die gesamte Embryonalentwicklung außerhalb des Muttertiers stattfindet. Daher ist besonders das Haushuhn im embryonalen Status für entwicklungsbiologische Studien geeignet. Der Dottersack des sich entwickelnden Embryos spielt dabei in Nahrungstransportprozessen eine tragende Rolle. Der Dottersack arbeitet als eine Form von Verdauungssystem, das Nährstoffe aus dem vom Dottersack umschlossenen Dotter aufnimmt. Der Dottersack ist aus 2 unterschiedlichen Zelltypen aufgebaut. Die untere, dem Dotter zugewandte Schicht, besteht aus einem Epithel aus endodermalen Zellen. Diese nehmen für den Embryo essentielle Nährstoffe aus dem Dotter auf. Direkt den endodermalen Epithelzellen aufsitzend befindet sich die zweite Zellschicht, die mesodermale Schicht aus einem Blutgefäß-Endothel, das Nährstoffe zum Embryo hin transportiert. Mit fortschreitender Entwicklung wird durch das Überwachsen der endodermalen Epithelschicht von dem mesodermalen Endothel die sogenannte area vasculosa gebildet. Jedoch enthält der Dottersack in den ersten Tagen nach der Eiablage große Bereiche von endodermalen Epithelzellen, die nicht von dem mesodermalen Endothel überzogen sind, welche als area vitellina bezeichnet werden.

In dieser Studie fand ich heraus, dass die endodermalen Epithelzellen der area vitellina einen großen Einfluss auf die intrazelluläre Fettspeicherung in sogenannten lipid droplets (LDs) haben. Diese Organellen, für die Versorgung des Embryos bereitgestellt, beinhalten zum Großteil neutrale Fette, wie Triglyzeride und Cholesterinester, und sind von einer Phospholipid Monoschicht begrenzt.

Ich entdeckte mit Hilfe von qPCR, dass der mRNA Spiegel von PLIN2, einem Mitglied einer LD-assoziierten Protein Familie, der perilipins (PLINs), im Dottersack stark erhöht war. Interessanterweise wiesen die nicht-vaskularisierten endodermalen Epithelzellen der area vitellina, und nicht die vaskularisierten Zellen der area vasculosa, erhöhte Expressionswerte auf. Bisher wurden im Modellorganismus Haushuhn die genauen Funktionen von PLIN2 noch nicht beschrieben. In Säugetieren hingegen wurde herausgefunden, dass PLIN2 an wachsende LDs bindet und von großer Wichtigkeit in der Fettspeicherung ist. Andere PLINs konnten in meinen Untersuchungen nicht detektiert werden.

Mit Hilfe der Western blot Technik konnte ich PLIN2 auch auf Proteinebene in der area vitellina nachweisen. Dies lässt auf eine wichtige Funktion von PLIN2 in der Fettspeicherung

schließen. Die direkte Assoziation von PLIN2 mit LDs konnte ich in der area vitellina mit einem α -PLIN2 Antikörper mittels Immunofärbung und Konfokalmikroskopie nachweisen.

Nachdem ich das Protein, welches mit großer Wahrscheinlichkeit für die Fettspeicherung im Dottersack verantwortlich ist, gefunden hatte, wollte ich herausfinden, wie die Lipide für Verwertung durch den Embryo mobilisiert werden können. Ich suchte nach einem Lipid-hydrolysierendem Enzym, das eine Spezifität für Triglyzerid-Spaltung hat, da dies der Ausgangspunkt für den Abbau von gespeicherten Fetten ist. Ich untersuchte die mRNS von mehreren Triglyzeridspaltenden Enzymen, und konnte tatsächlich eines, mit der Bezeichnung Patatin-like phospholipase domain-containing protein (PNPLA3), entdecken. Die höchsten PNPLA3 mRNS Spiegel wurden in den metabolisch aktiven Zellen der area vasculosa gemessen, also genau dort, von wo aus mit Hilfe der mesodermalen Blutgefäße Nährstoffe zum Embryo transportiert werden.

Acknowledgements

Jetzt, da meine Studienzeit zu Ende geht, muss ich unweigerlich einen Blick zurück auf das bisher erlebte und geleistete werfen. Noch sehr nahe scheint der Tag, an dem ich mich entschieden habe Biologie zu studieren und bis heute kann ich mit Gewissheit sagen, dass es die richtige Entscheidung war. Nachdem die anfängliche positive Nervosität, die „das Neue“ meist mit sich bringt verflogen war, hieß es sich auf den anspruchsvollen Studienalltag einzustellen. Doch auch dieser erwies sich stets als sehr abwechslungsreich und interessant für mich, nicht zuletzt auch wegen der vielen netten und guten Bekanntschaften die ich in den letzten Jahren gemacht habe.

Lange Rede kurzer Sinn: Ich habe die Studienzeit sehr genossen und würde im Nachhinein nichts ändern, auch wenn man nachher immer etwas schlauer ist und man hier und da vielleicht noch etwas mehr hätte lernen können. ;)

Doch all die wunderbaren Erfahrungen wären nicht möglich gewesen, wenn ich nicht die volle Unterstützung meiner Eltern gehabt hätte und damit meine ich nicht nur die Unterstützung mit der Bewältigung der nicht unerheblichen Unkosten eines Studiums. Besonders das Gefühl, in einem zu Hause zu leben, in dem man immer willkommen ist, bedeutet mir sehr viel. Hierbei möchte ich auch meine Schwester erwähnen, die mich immer durch ihre fröhliche und warmherzige Natur beeindruckt hat und mir so manches Mal mit guten Gesprächen weitergeholfen hat.

Verbunden mit dieser Master-Arbeit, möchte ich meinem offiziellen Betreuer Prof. Dr. Wolfgang J. Schneider danken, der mir die Möglichkeit gegeben hat, in so einem interessanten Forschungsgebiet Erfahrungen zu sammeln. Nie hätte ich mir vor dieser Laborarbeit gedacht, dass ich je einmal an *G. gallus domesticus* forschen würde. Um jedoch überhaupt präsentierbare Ergebnissen hervorzubringen, war im Labor besonders mein direkter Ansprechpartner Raimund von unschätzbarem Wert. Als hätte er nicht schon selbst genug mit seiner Doktorarbeit zu tun, war er immer voller neuer Ideen und hatte stets ein offenes Ohr für etwaige Anliegen und neue Vorschläge. Zusätzlich möchte ich noch kurz alle anderen lieben Leute aus dem Nimpf, Schneider und Hermann Labor nennen, die ebenfalls dazu beigetragen haben, dass die Laborarbeit stets positiv in Erinnerung bleiben wird.

Nicht zuletzt möchte ich auch meine Freundin Ines erwähnen, die mir immer wieder, in teilweise stressvollen Situationen zur Seite steht und mit der ich auch sonst immer schöne Zeiten verbringe.

Curriculum Vitae

Thomas Finkes

Personal Data

Name	Thomas Finkes
Address	Hauptstrasse 43a, 3422 Altenberg, Niederösterreich
Date of Birth	April 3 rd , 1986
Place of Birth	Vienna, Austria
Nationality	Austria

Education

10/2011 – 06/2012	Medical University of Vienna/MFPL/University of Vienna
Master thesis	Department of Medical Biochemistry, Division of Molecular Genetics, Lab of o. Univ. Prof. Dr. Wolfgang J. Schneider Title: "Molecular characterization of lipid droplet associated proteins in the chicken yolk sac"
03/2010 –	University of Vienna Master of Science in Molecular Biology, Faculty of Life Sciences with main focus on Molecular Medicine
10/2006 – 02/2010	University of Vienna Bachelor of Science in Microbiology and Genetics, Faculty of Life Sciences
09/1997 – 05/2005	Bundesgymnasium/Bundesrealgymnasium Klosterneuburg Main focus on Natural Sciences

Additional skills

Languages

German: Native language

English: Proficient

Spanish: Basic knowledge

Computer skills

Windows XP and 7: MS Office

Online biological databases (PubMed, Ensembl, EMBOSS, Ebi)

Basic skills with Adobe Photoshop

Employments

University of Vienna, Department of Chromosome Biology, Lab of Univ.-Prof. Dr. Franz Klein; Laboratory technician, 10/2008-10/2011

Poster

Raimund Bauer, Thomas Finkes, and Wolfgang J. Schneider. Lipoprotein Transport in the yolk sac. 19th annual meeting of the Austrian Atherosclerosis Society; St. Gilgen 2012.